Computer Assisted Mechanics and Engineering Sciences, **14**: 431–456, 2007.


# An overview of selected plate and shell FE models with graphic presentation of governing relations

Maria Radwańska
*Cracow University of Technology, Institute of Computational Civil Engineering, Cracow, Poland*

(Received July 5, 2005)

A survey of three forms (strong, weak and variational) of mathematical models is presented using expressive diagrams initiated in [3,10]. The primary and intermediate variables, governing field equations, constraint equations and variables specified by boundary conditions are components of the graphic representation of various FE (finite element) formulations. The attention is focused on linearly elastic plate element QUAD [9] for Mindlin–Reissner theory and shell elements EAS4-ANS, EAS7-ANS [1] based on CBRST (Continuum Based Resultant Shell Theory). In both cases the mixed FE models with the EAS (enhanced assumed strain) and ANS (assumed natural strain) concepts are used.

## 1. Introduction

The first step of finite element (FE) computer simulation is an idealization the basic idea of which consists in the mathematical modelling of a physical system. There are three mathematical forms of description of relevant boundary value problems (BVP) in linear elasticity: (i) a strong form (SF) recorded as a system of differential and algebraic equations, complemented by boundary conditions, (ii) a weak form (WF) defined by weighted residual integral equations, (iii) a variational form (VF) presented by appropriate functionals with their stationarity conditions. In view of both the theoretical and computational aspects, the relationships and transformations between these forms are essential [3]. The three mathematical forms (SF, WF, VF) can be converted into one another. The so-called Euler equations ensuing from the stationarity conditions of a particular functional correspond to specified differential or algebraic equations of the strong formulation. In many cases Green's theorem is used to perform integration by parts and to replace one form by an alternative statement. On the basis of integral residuals, having replaced weight functions by the variations of relevant variables, the components of functional stationarity condition are obtained.

Taking into account the discretization process and one-, two- or three-field FE approximation, the appropriate integral form can be transformed into a matrix algebraic equation system. The three alternative approaches may be used as the basis for the formulation of different FE types. All forms (strong, weak and variational) are presented in [3] by schemes, introduced by a mathematician E. Tonti, which are a graphic representation of the different approaches. A very complete description of the physical behaviour of thin plate structures was obtained [3] by the application of the strong form of field equations of the Kirchhoff plate theory together with weak formulations connected with one- and two-field variational principles. In various diagrams the corresponding equations can be found at the same point, following their interpretation. This is important for understanding both the relations between the variables describing the problem and the correspondence between various formulations as well. What the diagrams show clearly are the relations between all variables and equations in algebraic, differential or integral forms. For instance, with the Tonti diagrams the field equations for elastostatics, electrostatics or magnetostatics can be presented in a convenient graphic form.

The present paper is devoted to the application of graphic diagrams similar to Tonti [3] and Wiberg [10], regarding certain formulations of boundary value problems (BVP) related to two structure types:

(i) thin and moderately thick plate structures in which transverse shear effects are included (Mindlin–Reissner model),

(ii) thin and moderately thick shell structures with membrane, bending and transverse shear states.

The description of different formulations provided by relevant equations or in graphic diagrams can be treated as a starting point to the presentation of FE modelling also in a diagram. It is worth emphasizing that the FE description of plate/shell structures can be improved substantially by using finite elements based on the EAS (enhanced assumed strain) and ANS (assumed natural strain) methods [1, 9, 11]. The relations between shell theories and the formulation of degenerated shell finite elements are discussed in [4]. Paper [5] surveys FE models for the analysis of moderately thick shells on the basis of earlier works, while paper [6] is devoted to the presentation of energy functionals with the employment of conceptual diagrams for one-, two- and three-field and hybrid models. The main aim of the present paper is to enhance understanding of the EAS concept and the ANS method. The description of the EAS method is preceded by and confronted with general two- and three-field formulations (Sections 2–4). In the two-field formulation of the EAS method, beside the displacement approximation and strains compatible with it, an additional enhanced strain field is used. There is also a three-field EAS concept with the approximation of displacement, enhanced assumed strain and stress fields.

To visualize all details of the EAS formulation the graphic representation of basic formulae is shown in the paper (cf. Section 3.4) on new diagrams following Tonti's approach. A detailed description of two FEs chosen from literature,

(i) Mindlin–Reissner plate element QUAD [5],

(ii) plate/shell elements EAS4-ANS, EAS7-ANS [1],

is presented (cf. Sections 5 and 6).

The matrices and vectors for the two selected FEs, defined by relevant formulae, are illustrated in corresponding equations in the diagrams (cf. Sections 5.3.3 and 6.2–6.5). The interpretation of equations is simplified because analogous relations occupy the same place in all the diagrams corresponding to different approaches.

## 2. Three-field formulation ($\mathbf{u} - \boldsymbol{\sigma} - \boldsymbol{\varepsilon}$)

To visualize various approaches: (i) strong formulation, (ii) weighted residual method, (iii) variational principle, (iv) FE modelling, given by corresponding equations written below, four diagrams are shown in Figs. 1–4. The displacement, strain and stress fields are considered as three master (primary) fields, the relationships written as differential equations (with operator matrices), algebraic matrix equations or integral statements. In the diagrams strong and weak links are introduced. The strong form states the conditions that must be met at every material point, whereas the weak form states the conditions that must be satisfied only in an integral sense. Following discretization, in the three-field FE model three sets of degrees of freedom and three matrix equations are distinguished.

### 2.1. Strong formulation for elasticity problem

The general form of the three-field formulation for elasticity is given by the following set of equations, where the widely known abbreviations are used: Kinematic ($KE$), Constitutive ($CE$) and

Balance (equilibrium) (*BE*) Equations, Kinematic (*KBCs*) and Force static (*FBCs*) Boundary Conditions,

$$KE: \quad \boldsymbol{\varepsilon} = \mathbf{L}\mathbf{u}, \qquad \text{in } \Omega, \tag{1}$$

$$CE: \quad \boldsymbol{\sigma} = \mathbf{D}\boldsymbol{\varepsilon}, \qquad \text{in } \Omega, \tag{2}$$

$$BE: \quad \mathbf{L}^T\boldsymbol{\sigma} + \hat{\mathbf{p}} = \mathbf{0}, \qquad \text{in } \Omega, \tag{3}$$

$$KBCs: \quad \mathbf{u} = \hat{\mathbf{u}}, \qquad \text{on } \partial\Omega_u, \tag{4}$$

$$FBCs: \quad \mathbf{t} = \mathbf{n}\boldsymbol{\sigma} = \hat{\mathbf{t}}, \qquad \text{on } \partial\Omega_s. \tag{5}$$

The three fields of displacements $\mathbf{u}$, strains $\boldsymbol{\varepsilon}$ and stresses $\boldsymbol{\sigma}$ in the above set of equations, assumed in this formulation as master variables, together with the relations between them are shown in the expanded diagram in Fig. 1. Each strong connection corresponds to each equation and is drawn as a solid line.

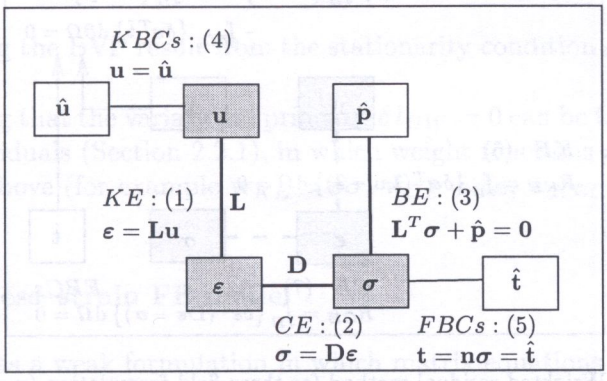


**Fig. 1.** Expanded Tonti diagram for elasticity problem according to strong formulation

## 2.2. Weak formulation

The investigation of an approximate solution of the BVP is performed within a weak formulation of this problem. Below two approaches related to the strong formulation, presented in the previous section, are discussed.

### *2.2.1. Weighted Residual Method*

As an alternative to the strong formulation it is possible to define two weak link residuals

$$\mathbf{r}_{KE} = \mathbf{L}\mathbf{u} - \boldsymbol{\varepsilon}, \qquad \mathbf{r}_{CE} = \mathbf{D}\boldsymbol{\varepsilon} - \boldsymbol{\sigma},$$

associated with kinematic and constitutive equations. Taking into account „work-conjugate" the appropriate weight functions

$$\mathbf{w}_{KE} = \delta\boldsymbol{\sigma}, \qquad \mathbf{w}_{CE} = \delta\boldsymbol{\varepsilon},$$

the integrated residuals are written as

$$R_{KE} = \int_\Omega \{\delta\boldsymbol{\sigma}^T(\mathbf{L}\mathbf{u} - \boldsymbol{\varepsilon})\}\,\mathrm{d}\Omega = 0, \tag{6}$$

$$R_{CE} = \int_\Omega \{\delta\boldsymbol{\varepsilon}^T(\mathbf{D}\boldsymbol{\varepsilon} - \boldsymbol{\sigma})\}\,\mathrm{d}\Omega = 0. \tag{7}$$

Additionally, the virtual work principle (*VWP*) is represented by the equation

$$\delta W_{int} + \delta W_{ext} = \int_{\Omega} \{\delta \boldsymbol{\varepsilon}^T \boldsymbol{\sigma}\} \, \mathrm{d}\Omega - \int_{\Omega} \{\delta \mathbf{u}^T \hat{\mathbf{p}}\} \, \mathrm{d}\Omega - \int_{\partial\Omega_s} \{\delta \mathbf{u}^T \hat{\mathbf{t}}\} \, \mathrm{d}\partial\Omega = 0. \tag{8}$$

The equation is valid for virtual deformation (virtual displacement satisfying constraint $\delta \mathbf{u} = \mathbf{0}$ on $\partial\Omega_u$ and virtual strain connected with the virtual displacement by kinematic relation $\delta\boldsymbol{\varepsilon} = \mathbf{L}\delta\mathbf{u}$) and for the real stress field represented by $\boldsymbol{\sigma}$ and $\hat{\mathbf{t}}$. The virtual work statement is the weak form of the equilibrium equations and is valid for both linear and nonlinear constitutive relations. The corresponding diagram (Fig. 2) shows weakened connections related to the weighted residual method. The kinematic boundary conditions are omitted in Fig. 2.

The weighted residual variational approach can often be treated as a starting point for the generalization of FE concepts.

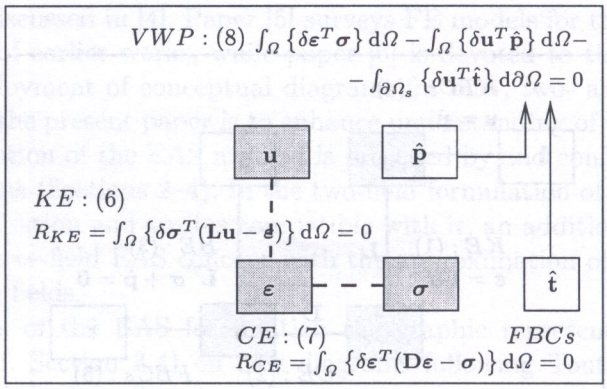


**Fig. 2.** Weighted residual method for three-field formulation ($\mathbf{u} - \boldsymbol{\sigma} - \boldsymbol{\varepsilon}$)

### *2.2.2. Hu–Washizu principle*

The Hu–Washizu variational functional is referred to three primary fields $\mathbf{u}$, $\boldsymbol{\sigma}$, $\boldsymbol{\varepsilon}$ (which are defined in $\Omega$ and free from any constraints) and additionally to tractions $\mathbf{t}$ introduced on $\partial\Omega_u$ [11]

$$I_{HW}[\mathbf{u}, \boldsymbol{\sigma}, \boldsymbol{\varepsilon} \mid \mathbf{t}] = I_{int} - I_{ext} = \int_{\Omega} \left\{ \frac{1}{2} \boldsymbol{\varepsilon}^T \mathbf{D} \boldsymbol{\varepsilon} - \boldsymbol{\sigma}^T (\boldsymbol{\varepsilon} - \mathbf{L}\mathbf{u}) \right\} \mathrm{d}\Omega - \int_{\Omega} \{\mathbf{u}^T \hat{\mathbf{p}}\} \, \mathrm{d}\Omega$$
$$- \int_{\partial\Omega_s} \{\mathbf{u}^T \hat{\mathbf{t}}\} \, \mathrm{d}\partial\Omega - \int_{\partial\Omega_u} \{\mathbf{t}^T (\mathbf{u} - \hat{\mathbf{u}})\} \, \mathrm{d}\partial\Omega. \tag{9}$$

The stationarity condition for the functional $I_{HW}$,

$$\delta I_{HW}[\mathbf{u}, \boldsymbol{\sigma}, \boldsymbol{\varepsilon}, \mathbf{t}] = \frac{\partial I_{HW}}{\partial \mathbf{u}} \delta\mathbf{u} + \frac{\partial I_{HW}}{\partial \boldsymbol{\sigma}} \delta\boldsymbol{\sigma} + \frac{\partial I_{HW}}{\partial \boldsymbol{\varepsilon}} \delta\boldsymbol{\varepsilon} + \frac{\partial I_{HW}}{\partial \mathbf{t}} \delta\mathbf{t} = 0, \tag{10}$$

with the use of Green's theorem leads to the so-called Euler equations, which stand in $\Omega$ and $\partial\Omega_u$ or $\partial\Omega_s$, assuming a free choice of $\delta\mathbf{u}, \delta\boldsymbol{\sigma}, \delta\boldsymbol{\varepsilon}$ in $\Omega$, $\delta\mathbf{u}$ on $\partial\Omega_s$ and $\delta\mathbf{t}$ on $\partial\Omega_u$:

$$\bigwedge \delta\mathbf{u}: \quad \mathbf{L}^T\boldsymbol{\sigma} + \hat{\mathbf{p}} = \mathbf{0} \quad (a) \quad \text{in } \Omega, \qquad \mathbf{t} = \hat{\mathbf{t}} \quad (b) \quad \text{on } \partial\Omega_\sigma, \quad \mathbf{n}\boldsymbol{\sigma} = \mathbf{t} \quad (c) \quad \text{on } \partial\Omega_u,$$
$$\bigwedge \delta\boldsymbol{\sigma}: \quad \boldsymbol{\varepsilon} = \mathbf{L}\mathbf{u}, \qquad (d) \quad \text{in } \Omega,$$
$$\bigwedge \delta\boldsymbol{\varepsilon}: \quad \boldsymbol{\sigma} = \mathbf{D}\boldsymbol{\varepsilon} \qquad (e) \quad \text{in } \Omega,$$
$$\bigwedge \delta\mathbf{t}: \quad \mathbf{u} = \hat{\mathbf{u}} \qquad (f) \quad \text{on } \partial\Omega_u,$$

with $\delta\mathbf{u} = \mathbf{0}$ on $\partial\Omega_u$ and $\delta\boldsymbol{\sigma} = \mathbf{0}$ on $\partial\Omega_s$.

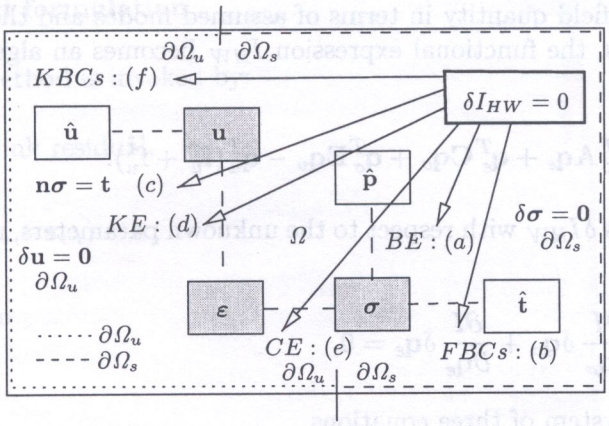


**Fig. 3.** Weak form diagram for Hu–Washizu principle $(\mathbf{u} - \boldsymbol{\sigma} - \boldsymbol{\varepsilon})$

All relations describing the BVP result from the stationarity condition $\delta I_{HW} = 0$, and are shown in Fig. 3.

It is worth emphasizing that the variational principle $\delta I_{HW} = 0$ can be formulated by the addition of relevant integrated residuals (Section 2.2.1), in which weight functions are replaced by variations of appropriate fields as above (for example $\mathbf{w}_{KE} = \delta\boldsymbol{\sigma}$, $\mathbf{w}_{CE} = \delta\boldsymbol{\varepsilon}$, $\mathbf{w}_{KBC} = \delta\mathbf{t}$ or $\mathbf{w}_{FBC} = \delta\mathbf{u}$) [3].

## 2.3. Displacement–stress–strain FE model

FE modelling is treated as a weak formulation in which matrix equations describe the interconnections between appropriate fields, represented by the vectors of degrees of freedom (DOFs). The FE models diagrams (Fig. 4) illustrate both the approximated fields and vectors of DOFs, treated as master unknowns, introduced in FE approximation.

The equations of a three-field FE model are related to the approximation of three primary fields

$$\mathbf{u} = \mathbf{N}_u\mathbf{q}_u, \qquad \boldsymbol{\sigma} = \mathbf{N}_\sigma\mathbf{q}_\sigma, \qquad \boldsymbol{\varepsilon} = \mathbf{N}_\varepsilon\mathbf{q}_\varepsilon \tag{11}$$

and to the Hu–Washizu functional.

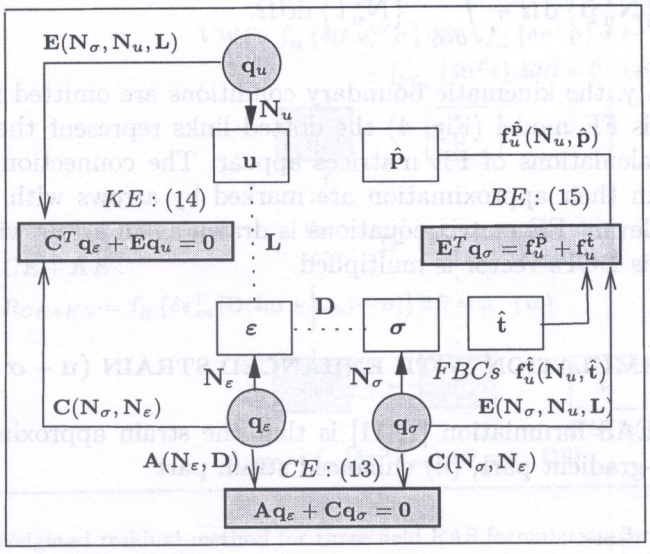


**Fig. 4.** Three-field FE model $(\mathbf{u} - \boldsymbol{\sigma} - \boldsymbol{\varepsilon})$

Having expressed the field quantity in terms of assumed modes and their associated DOFs, and following the integrations, the functional expression $I_{HW}$ becomes an algebraic function of a finite number of DOFs

$$I_{HW}[\mathbf{q}_u, \mathbf{q}_\sigma, \mathbf{q}_\varepsilon] = \frac{1}{2}\mathbf{q}_\varepsilon^T \mathbf{A}\mathbf{q}_\varepsilon + \mathbf{q}_\varepsilon^T \mathbf{C}\mathbf{q}_\sigma + \mathbf{q}_\sigma^T \mathbf{E}\mathbf{q}_u - \mathbf{q}_u^T(\mathbf{f}_u^{\hat{\mathbf{p}}} + \mathbf{f}_u^{\hat{\mathbf{t}}}). \tag{12}$$

Calculating the variations $\delta I_{HW}$ with respect to the unknown parameters, according to the standard procedure

$$\delta I_{HW} = \frac{\partial I}{\partial \mathbf{q}_u}\delta\mathbf{q}_u + \frac{\partial I}{\partial \mathbf{q}_\sigma}\delta\mathbf{q}_\sigma + \frac{\partial I}{\partial \mathbf{q}_\varepsilon}\delta\mathbf{q}_\varepsilon = 0,$$

results in the following system of three equations

$$\bigwedge \delta\mathbf{q}_\varepsilon : \quad CE: \quad \mathbf{A}\mathbf{q}_\varepsilon + \mathbf{C}\mathbf{q}_\sigma + \mathbf{0}\mathbf{q}_u = \mathbf{0}, \tag{13}$$

$$\bigwedge \delta\mathbf{q}_\sigma : \quad KE: \quad \mathbf{C}^T\mathbf{q}_\varepsilon + \mathbf{0}\mathbf{q}_\sigma + \mathbf{E}\mathbf{q}_u = \mathbf{0}, \tag{14}$$

$$\bigwedge \delta\mathbf{q}_u : \quad BE: \quad \mathbf{0}^T\mathbf{q}_\varepsilon + \mathbf{E}^T\mathbf{q}_\sigma + \mathbf{0}\mathbf{q}_u = \mathbf{f}_u^{\hat{\mathbf{p}}} + \mathbf{f}_u^{\hat{\mathbf{t}}}, \tag{15}$$

written additionally in a matrix form

$$\begin{bmatrix} \mathbf{A} & \mathbf{C} & \mathbf{0} \\ \mathbf{C}^T & \mathbf{0} & \mathbf{E} \\ \mathbf{0} & \mathbf{E}^T & \mathbf{0} \end{bmatrix} \begin{bmatrix} \mathbf{q}_\varepsilon \\ \mathbf{q}_\sigma \\ \mathbf{q}_u \end{bmatrix} = \begin{bmatrix} \mathbf{0} \\ \mathbf{0} \\ \mathbf{f}_u^{\hat{\mathbf{p}}} + \mathbf{f}_u^{\hat{\mathbf{t}}} \end{bmatrix}.$$

The following matrices and vectors are used above:

$$\mathbf{A} = \mathbf{A}_{\varepsilon\varepsilon} = \int_{\Omega_e} \{\mathbf{N}_\varepsilon^T \mathbf{D}\mathbf{N}_\varepsilon\}\, \mathrm{d}\Omega,$$

$$\mathbf{C} = \mathbf{C}_{\varepsilon\sigma} = -\int_{\Omega_e} \{\mathbf{N}_\varepsilon^T \mathbf{N}_\sigma\}\, \mathrm{d}\Omega,$$

$$\mathbf{E} = \mathbf{E}_{\sigma u} = \int_{\Omega_e} \{\mathbf{N}_\sigma^T (\mathbf{L}\mathbf{N}_u)\}\, \mathrm{d}\Omega,$$

$$\mathbf{f}_u = \mathbf{f}_u^{\hat{\mathbf{p}}} + \mathbf{f}_u^{\hat{\mathbf{t}}} = \int_{\Omega_e} \{\mathbf{N}_u^T \hat{\mathbf{p}}\}\, \mathrm{d}\Omega + \int_{\partial\Omega_{e,s}} \{\mathbf{N}_u^T \hat{\mathbf{t}}\}\, \mathrm{d}\partial\Omega.$$

For the sake of simplicity, the kinematic boundary conditions are omitted in the equations. In the diagrams describing this FE model (Fig. 4) the dotted links represent the relations in which the matrices used in the calculations of FE matrices appear. The connection between variables and vectors of DOFs used in their approximation are marked by arrows with full heads. Inclusion of each DOFs vector in relevant FE matrix equations is drawn as an arrow with empty head, next to the matrix by which this DOFs vector is multiplied.

## 3. Three-field formulation with enhanced strain ($\mathbf{u} - \sigma - \varepsilon_{EN}$)

The main idea of the EAS formulation [1, 11] is that the strain approximation is split into two terms: (i) displacement-gradient part, (ii) enhanced strain part

$$\varepsilon = \varepsilon_u + \varepsilon_{en} = \mathbf{L}\mathbf{u} + \varepsilon_{en}. \tag{16}$$

As in Sec. 2.2, the two variants of weak formulation are presented briefly below.

### 3.1. Weighted residual formulation

The weighted residual method is invoked by:

(i) the following weak link residual,

$$\mathbf{r}_{KE+CE} = \mathbf{D}(\mathbf{L}\mathbf{u} + \boldsymbol{\varepsilon}_{en}) - \boldsymbol{\sigma}, \tag{17}$$

with weight function

$$\mathbf{w} = \delta\boldsymbol{\varepsilon}_{en}$$

and integral residual related to the couple of kinematic and constitutive equations

$$R_{CE+KE} = \int_{\Omega} \left\{\delta\boldsymbol{\varepsilon}_{en}^{T} \left[\mathbf{D}(\mathbf{L}\mathbf{u} + \boldsymbol{\varepsilon}_{en}) - \boldsymbol{\sigma}\right]\right\} \mathrm{d}\Omega = 0, \tag{18}$$

(ii) integral orthogonality condition, ensuing from the EAS formulation

$$I_{ORT} = \int_{\Omega} \left\{\delta\boldsymbol{\sigma}^{T}\boldsymbol{\varepsilon}_{en}\right\} \mathrm{d}\Omega = 0, \tag{19}$$

(iii) virtual work statement

$$\int_{\Omega} \left\{\delta(\mathbf{L}\mathbf{u})^{T}\boldsymbol{\sigma}\right\} \mathrm{d}\Omega - \int_{\Omega} \left\{\delta\mathbf{u}^{T}\hat{\mathbf{p}}\right\} \mathrm{d}\Omega - \int_{\partial\Omega_s} \left\{\delta\mathbf{u}^{T}\hat{\mathbf{t}}\right\} \mathrm{d}\partial\Omega = 0. \tag{20}$$

The above relations are shown in Fig. 5 as links between relevant unknown and prescribed variables.

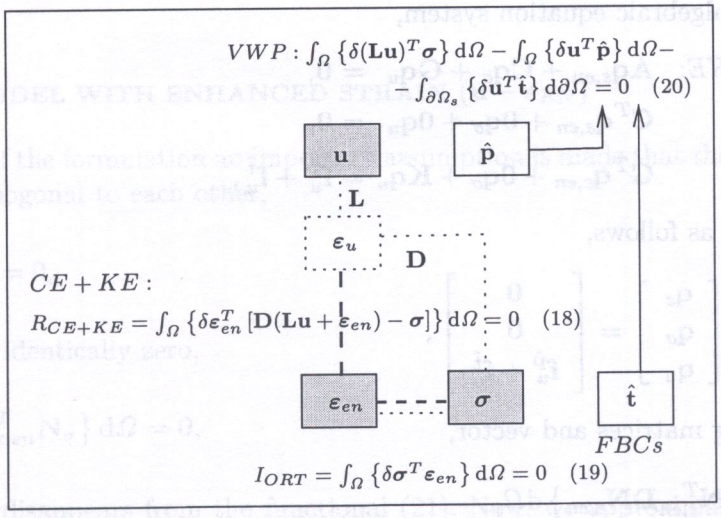


**Fig. 5.** Weighted residual method for three field EAS formulation ($\mathbf{u} - \boldsymbol{\sigma} - \boldsymbol{\varepsilon}_{en}$)

### 3.2. Modified Hu–Washizu principle

The EAS approach is based on the variational principle which is related to the stationarity of the modified Hu–Washizu functional, dependent on three fields: displacements, stresses and enhanced strains

$$I^{(3)}_{HWen}[\mathbf{u},\boldsymbol{\sigma},\boldsymbol{\varepsilon}_{en}] = \int_{\Omega}\left\{\frac{1}{2}(\mathbf{Lu}+\boldsymbol{\varepsilon}_{en})^T\mathbf{D}(\mathbf{Lu}+\boldsymbol{\varepsilon}_{en})\right\}\mathrm{d}\Omega - \int_{\Omega}\{\boldsymbol{\sigma}^T\boldsymbol{\varepsilon}_{en}\}\,\mathrm{d}\Omega$$
$$- \int_{\Omega}\{\mathbf{u}^T\hat{\mathbf{p}}\}\,\mathrm{d}\Omega - \int_{\partial\Omega_s}\{\mathbf{u}^T\hat{\mathbf{t}}\}\,\mathrm{d}\partial\Omega \tag{21}$$
$$\rightarrow \quad \delta I^{(3)}_{HWen} = \frac{\partial I_{HW}}{\partial \mathbf{u}}\,\delta\mathbf{u} + \frac{\partial I_{HW}}{\partial \boldsymbol{\sigma}}\,\delta\boldsymbol{\sigma} + \frac{\partial I_{HW}}{\partial \boldsymbol{\varepsilon}_{en}}\,\delta\boldsymbol{\varepsilon}_{en} = 0.$$

### 3.3. The three-field ($\mathbf{u}-\boldsymbol{\sigma}-\boldsymbol{\varepsilon}_{en}$) FE model

In the EAS model the approximation is applied to $\mathbf{u},\boldsymbol{\sigma},\boldsymbol{\varepsilon}$ fields

$$\mathbf{u} = \mathbf{N}_u\mathbf{q}_u, \qquad \boldsymbol{\sigma} = \mathbf{N}_\sigma\mathbf{q}_\sigma, \qquad \boldsymbol{\varepsilon}_{en} = \mathbf{N}_{\varepsilon,en}\mathbf{q}_{\varepsilon,en}\,, \tag{22}$$

with a special treatment of the strain field, with introduction of the extra enhanced strains $\boldsymbol{\varepsilon}_{en}$, beside the component of strains $\boldsymbol{\varepsilon}_u$ resulting from the displacement field

$$\boldsymbol{\varepsilon}_u = \mathbf{L}\mathbf{N}_u\mathbf{q}_u\,.$$

The additional enhanced strain field can also be presented as a product of interpolation matrix $\mathbf{M}$ and internal (not nodal) strain parameters $\boldsymbol{\alpha}$

$$\boldsymbol{\varepsilon}_{en} = \mathbf{M}\boldsymbol{\alpha}.$$

The stationarity requirement for functional $I_{HWen}$ which can be written as a function of DOFs vectors

$$I^{(3)}_{HWen}[\mathbf{q}_u,\mathbf{q}_\sigma,\mathbf{q}_{\varepsilon,en}] = \frac{1}{2}\mathbf{q}_u^T\mathbf{K}\mathbf{q}_u + \frac{1}{2}\mathbf{q}_{\varepsilon,en}^T\mathbf{A}\mathbf{q}_{\varepsilon,en} + \mathbf{q}_{\varepsilon,en}^T\mathbf{G}\mathbf{q}_u + \mathbf{q}_{\varepsilon,en}^T\mathbf{C}\mathbf{q}_\sigma - \mathbf{q}_u^T(\mathbf{f}_u^{\hat{\mathbf{p}}} + \mathbf{f}_u^{\hat{\mathbf{t}}}) \tag{23}$$
$$\rightarrow \quad \delta I^{(3)}_{HWen} = 0,$$

yields the following algebraic equation system,

$$\bigwedge \delta\mathbf{q}_{\varepsilon,en}: \quad CE{+}KE: \quad \mathbf{A}\mathbf{q}_{\varepsilon,en} + \mathbf{C}\mathbf{q}_\sigma + \mathbf{G}\mathbf{q}_u = \mathbf{0}, \tag{24}$$
$$\bigwedge \delta\mathbf{q}_\sigma: \quad ORT: \quad \mathbf{C}^T\mathbf{q}_{\varepsilon,en} + \mathbf{0}\mathbf{q}_\sigma + \mathbf{0}\mathbf{q}_u = \mathbf{0}, \tag{25}$$
$$\bigwedge \delta\mathbf{q}_u: \quad BE: \quad \mathbf{G}^T\mathbf{q}_{\varepsilon,en} + \mathbf{0}\mathbf{q}_\sigma + \mathbf{K}\mathbf{q}_u = \mathbf{f}_u^{\hat{\mathbf{p}}} + \mathbf{f}_u^{\hat{\mathbf{t}}}, \tag{26}$$

with its matrix form as follows,

$$\begin{bmatrix} \mathbf{A} & \mathbf{C} & \mathbf{G} \\ \mathbf{C}^T & \mathbf{0} & \mathbf{0} \\ \mathbf{G}^T & \mathbf{0} & \mathbf{K} \end{bmatrix}\begin{bmatrix} \mathbf{q}_\varepsilon \\ \mathbf{q}_\sigma \\ \mathbf{q}_u \end{bmatrix} = \begin{bmatrix} \mathbf{0} \\ \mathbf{0} \\ \mathbf{f}_u^{\hat{\mathbf{p}}} + \mathbf{f}_u^{\hat{\mathbf{t}}} \end{bmatrix},$$

defining the following matrices and vector,

$$\mathbf{A} = \mathbf{A}_{\varepsilon\varepsilon} = \int_{\Omega_e}\{\mathbf{N}_{\varepsilon,en}^T\mathbf{D}\mathbf{N}_{\varepsilon,en}\}\,\mathrm{d}\Omega,$$
$$\mathbf{C} = \mathbf{C}_{\varepsilon\sigma} = -\int_{\Omega_e}\{\mathbf{N}_{\varepsilon,en}^T\mathbf{N}_\sigma\}\,\mathrm{d}\Omega,$$

$$\mathbf{G} = \mathbf{G}_{\varepsilon u} = \int_{\Omega_e} \{\mathbf{N}_{\varepsilon,en}^T \mathbf{D}(\mathbf{L}\mathbf{N}_u)\}\, \mathrm{d}\Omega,$$

$$\mathbf{K} = \mathbf{K}_{uu} = \int_{\Omega_e} \{(\mathbf{L}\mathbf{N}_u)^T \mathbf{D}(\mathbf{L}\mathbf{N}_u)\}\, \mathrm{d}\Omega,$$

$$\mathbf{f}_u = \mathbf{f}_u^{\hat{\mathbf{p}}} + \mathbf{f}_u^{\hat{\mathbf{t}}} = \int_{\Omega_e} \{\mathbf{N}_u^T \hat{\mathbf{p}}\}\, \mathrm{d}\Omega + \int_{\partial\Omega_{e,s}} \{\mathbf{N}_u^T \hat{\mathbf{t}}\}\, \mathrm{d}\partial\Omega.$$

It is important to note that in the diagrams in Figs. 5 and 6 two parts of the strain field are shown: (i) $\boldsymbol{\varepsilon}_u$ displacement-gradients dependent (secondary field) and (ii) additional enhanced $\boldsymbol{\varepsilon}_{en}$, treated as one of three master (primary) fields.

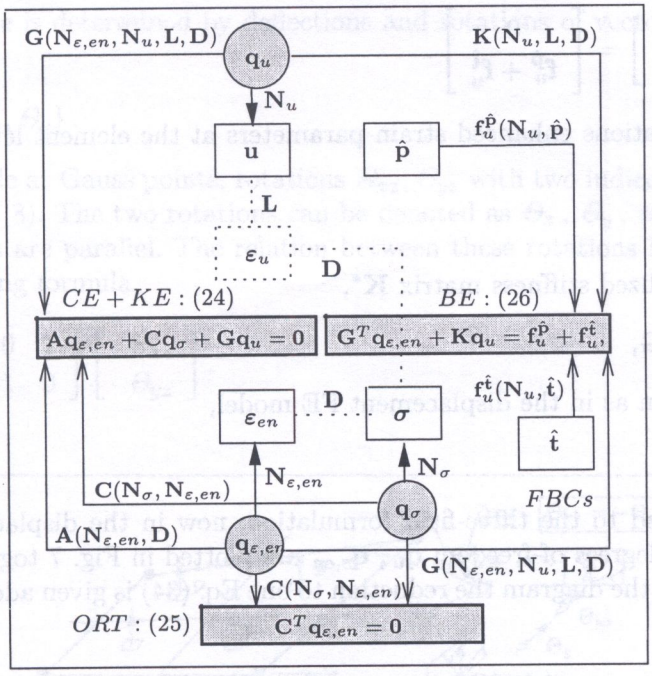


**Fig. 6.** Three-field FE model with EAS $(\mathbf{u} - \boldsymbol{\sigma} - \boldsymbol{\varepsilon}_{en})$

## 4. TWO-FIELD MODEL WITH ENHANCED STRAIN $(\mathbf{u} - \boldsymbol{\varepsilon}_{EN})$

In the next variant of the formulation an important assumption is made that the stress and enhanced strain fields are orthogonal to each other,

$$\int_{\Omega_e} \{\boldsymbol{\sigma}^T \boldsymbol{\varepsilon}_{en}\}\, \mathrm{d}\Omega = 0,$$

so that matrix $\mathbf{C}$ is identically zero,

$$\mathbf{C}_{\varepsilon\sigma} = -\int_{\Omega_e} \{\mathbf{N}_{\varepsilon,en}^T \mathbf{N}_\sigma\}\, \mathrm{d}\Omega = \mathbf{0}, \tag{27}$$

and the stress field disappears from the functional (21). Now, we approximate independently two fields, displacements $\mathbf{u}$ and enhanced strains $\boldsymbol{\varepsilon}_{en}$, as

$$\mathbf{u} = \mathbf{N}_u \mathbf{q}_u, \qquad \boldsymbol{\varepsilon}_{en} = \mathbf{N}_{\varepsilon,en} \mathbf{q}_{\varepsilon,en}\,. \tag{28}$$

Adopting the variational functional and principle

$$I^{(2)}_{HWen}[\mathbf{q}_u, \mathbf{q}_{\varepsilon,en}] = \frac{1}{2}\mathbf{q}_u^T\mathbf{K}\mathbf{q}_u + \frac{1}{2}\mathbf{q}_{\varepsilon,en}^T\mathbf{A}\mathbf{q}_{\varepsilon,en} + \mathbf{q}_{\varepsilon,en}^T\mathbf{G}\mathbf{q}_u - \mathbf{q}_u^T(\mathbf{f}_u^{\hat{\mathbf{p}}} + \mathbf{f}_u^{\hat{\mathbf{t}}}) \tag{29}$$

$$\rightarrow \delta I^{(2)}_{HWen}[\mathbf{q}_u, \mathbf{q}_{\varepsilon,en}] = 0,$$

the following matrix equations are obtained,

$$\bigwedge \delta\mathbf{q}_\varepsilon : \quad CE{+}KE\text{:} \quad \mathbf{A}\mathbf{q}_{\varepsilon,en} + \mathbf{G}\mathbf{q}_u = \mathbf{0}, \tag{30}$$

$$\bigwedge \delta\mathbf{q}_u : \quad BE\text{:} \quad \mathbf{G}^T\mathbf{q}_{\varepsilon,en} + \mathbf{K}\mathbf{q}_u = \mathbf{f}_u^{\hat{\mathbf{p}}} + \mathbf{f}_u^{\hat{\mathbf{t}}}, \tag{31}$$

written next in a matrix form

$$\begin{bmatrix} \mathbf{A} & \mathbf{G} \\ \mathbf{G}^T & \mathbf{K} \end{bmatrix} \begin{bmatrix} \mathbf{q}_{\varepsilon,en} \\ \mathbf{q}_u \end{bmatrix} = \begin{bmatrix} \mathbf{0} \\ \mathbf{f}_u^{\hat{\mathbf{p}}} + \mathbf{f}_u^{\hat{\mathbf{t}}} \end{bmatrix}.$$

In numerical applications enhanced strain parameters at the element level are frequently eliminated,

$$\mathbf{q}_{\varepsilon,en} = -\mathbf{A}^{-1}\mathbf{G}\mathbf{q}_u\,, \tag{32}$$

which gives the generalized stiffness matrix $\mathbf{K}^*$,

$$\mathbf{K}^* = \mathbf{K} - \mathbf{G}^T\mathbf{A}^{-1}\mathbf{G}, \tag{33}$$

and a compact equation as in the displacement FE model,

$$\mathbf{K}^*\mathbf{q}_u = \mathbf{f}_u\,. \tag{34}$$

Unlike Fig. 6, related to the three-field formulation, now in the displacement-enhanced strain FE model two sets of degrees of freedom $\mathbf{q}_u$ , $\mathbf{q}_{\varepsilon,en}$ are plotted in Fig. 7 toghether with two matrix equations (30)–(31). In the diagram the reduction to one Eq. (34) is given additionally at the bottom of the figure.

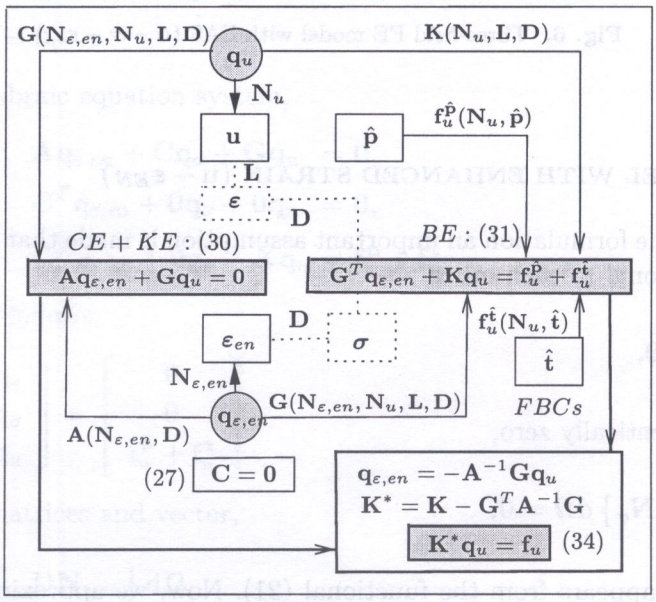


**Fig. 7.** Two-field FE model with EAS ($\mathbf{u} - \boldsymbol{\varepsilon}_{en}$)

## 5. Model problem I: Mindlin–Reissner plate element

The first problem discussed in detail in the paper is the presentation of new diagrams for:

(i) strong form of equations for the Mindlin–Reissner plate theory,

(ii) weak integral forms determined from relevant functionals and connected with the FE model.

Analogous diagrams describing the Kirchhoff plate can be found in [3].

### 5.1. Strong form of field equations

The deformation of plate is determined by deflections and rotations of vectors normal to the mid-surface

$$\mathbf{u} = \{w, \boldsymbol{\Theta}\} = \{w, \Theta_x, \Theta_y\}.$$

In domain $\Omega$, for example at Gauss points, rotations $\Theta_{xz}$, $\Theta_{yz}$ with two indices are defined in planes $(x,z)$ and $(y,z)$ (cf. Fig. 8). The two rotations can be denoted as $\Theta_x$, $\Theta_y$, according to the axis to which respective vectors are parallel. The relation between these rotations is shown in Fig. 8 and expressed by the following formula,

$$\boldsymbol{\Theta} = \begin{bmatrix} \Theta_x \\ \Theta_y \end{bmatrix} = \begin{bmatrix} 0 & 1 \\ -1 & 0 \end{bmatrix} \begin{bmatrix} \Theta_{xz} \\ \Theta_{yz} \end{bmatrix}.$$

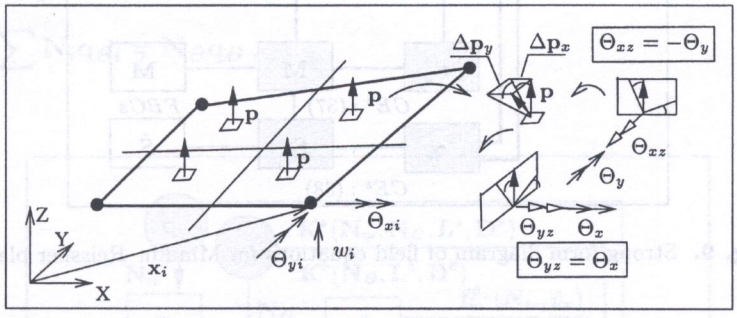


**Fig. 8.** FE model for Mindlin–Reissner plate

The *KE* and *CE* equations for first-order shear deformation plate theory are:

$$KE^b: \quad \boldsymbol{\kappa} = \boldsymbol{\kappa}^{\Theta} = \boldsymbol{\nabla}^b \boldsymbol{\Theta}, \qquad \boldsymbol{\nabla}^b = \begin{bmatrix} \frac{\partial}{\partial x} & 0 \\ 0 & \frac{\partial}{\partial y} \\ \frac{\partial}{\partial y} & \frac{\partial}{\partial x} \end{bmatrix}, \tag{35}$$

$$KE^s: \quad \boldsymbol{\gamma} = \boldsymbol{\gamma}^{w,\Theta} = \boldsymbol{\nabla} w - \boldsymbol{\Theta}, \qquad \boldsymbol{\nabla} = \begin{bmatrix} \frac{\partial}{\partial x} \\ \frac{\partial}{\partial y} \end{bmatrix}, \tag{36}$$

$$CE^b: \quad \mathbf{M} = \mathbf{D}^b \boldsymbol{\kappa}, \qquad \mathbf{D}^b = D_b \begin{bmatrix} 1 & \nu & 0 \\ \nu & 1 & 0 \\ 0 & 0 & (1-\nu)/2 \end{bmatrix}, \quad D_b = \frac{Et^3}{12(1-\nu^2)}, \tag{37}$$

$$CE^s: \quad \mathbf{S} = \mathbf{D}^s \boldsymbol{\gamma}, \qquad \mathbf{D}^s = D_s \begin{bmatrix} 1 & 0 \\ 0 & 1 \end{bmatrix}, \quad D_s = kGt. \tag{38}$$

Three equilibrium equations (*BE*) can be written as

$$(\nabla^b)^T\mathbf{M}+\mathbf{S}=\mathbf{0}, \qquad \nabla^T\mathbf{S}+\hat{p}_z=0. \tag{39}$$

For a thick plate independent specification of three boundary conditions from among: kinematic (*KBCs*)

$$KBCs: \qquad \Theta_n=\hat{\Theta}_n, \quad \Theta_s=\hat{\Theta}_s, \quad w=\hat{w}, \tag{40}$$

or force (static) (*FBCs*),

$$FBCs: \qquad M_{nn}=\hat{M}_{nn}, \quad M_{ns}=\hat{M}_{ns}, \quad S=\hat{S}, \tag{41}$$

or mixed boundary conditions (*MBCs*) is permitted at each point of the boundary.

The graphic presentation of the governing equations, including boundary conditions, related to the strong form of the problem, is given in the diagram in Fig. 9.

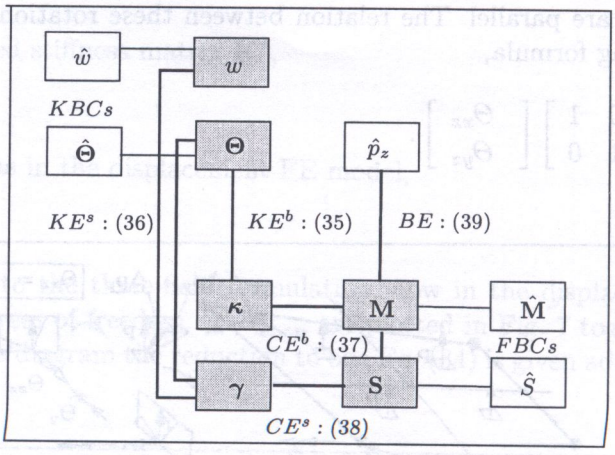


**Fig. 9.** Strong form diagram of field equations for Mindlin–Reissner plate

The behaviour of a moderately thick plate can also be described by the condensed sets of:

(i) displacement equations

$$(\nabla^b)^T\mathbf{D}^b\nabla^b\Theta+kGt(\nabla w-\Theta)=\mathbf{0}, \qquad \nabla^T[kGt(\nabla w-\Theta)]+\hat{p}_z=0, \tag{42}$$

(ii) mixed equations

$$(\nabla^b)^T\mathbf{D}^b\nabla^b\Theta+\mathbf{S}=\mathbf{0}, \qquad \mathbf{S}=kGt(\nabla w-\Theta), \qquad \nabla^T\mathbf{S}+\hat{p}_z=0. \tag{43}$$

### 5.2. Displacement FE model

The formulation is repeated here to show the differences between the original one-field displacement formulation and a mixed one, presented further in Sec. 5.3.

### *5.2.1. Variational form related to total potential energy functional*

In the total potential energy (TPE) functional there are only two master fields: transverse displacement and rotations of transverse normal (Fig. 9). Adopting the resultant stresses enables the separation of bending and shear states, which induces the introduction of the following parts of energy,

$$
\begin{aligned}
I_P[w,\boldsymbol{\Theta}] &= I_P^b + I_P^s - I_{ext} \\
&= \int_\Omega \left\{ \frac{1}{2} (\boldsymbol{\nabla}^b \boldsymbol{\Theta})^T \mathbf{D}^b (\boldsymbol{\nabla}^b \boldsymbol{\Theta}) \right\} \mathrm{d}\Omega + \int_\Omega \left\{ \frac{1}{2} (\boldsymbol{\nabla} w - \boldsymbol{\Theta})^T \mathbf{D}^s (\boldsymbol{\nabla} w - \boldsymbol{\Theta}) \right\} \mathrm{d}\Omega \\
&\quad - \int_\Omega \{ w \hat{p}_z \} \, \mathrm{d}\Omega - \int_{\partial\Omega_s} \left\{ w \hat{S} \right\} \mathrm{d}\partial\Omega - \int_{\partial\Omega_s} \left\{ \boldsymbol{\Theta}^T \hat{\mathbf{M}} \right\} \mathrm{d}\partial\Omega = 0,
\end{aligned} \tag{44}
$$

and the stationarity condition,

$$
\delta I_P^b + \delta I_P^s - \delta I_{ext} = 0,
$$

from which respective Euler equations are obtained.

### *5.2.2. Displacement FE model for bending and shear states*

The approximation of generalized displacements as master fields,

$$
\mathbf{u} = \{w\} = \sum \mathbf{N}_i \mathbf{q}_{wi} = \mathbf{N}_w \mathbf{q}_w, \tag{45}
$$

$$
\boldsymbol{\Theta} = \{\Theta_x \Theta_y\} = \sum \mathbf{N}_i \mathbf{q}_{\Theta i} = \mathbf{N}_\Theta \mathbf{q}_\Theta, \tag{46}
$$

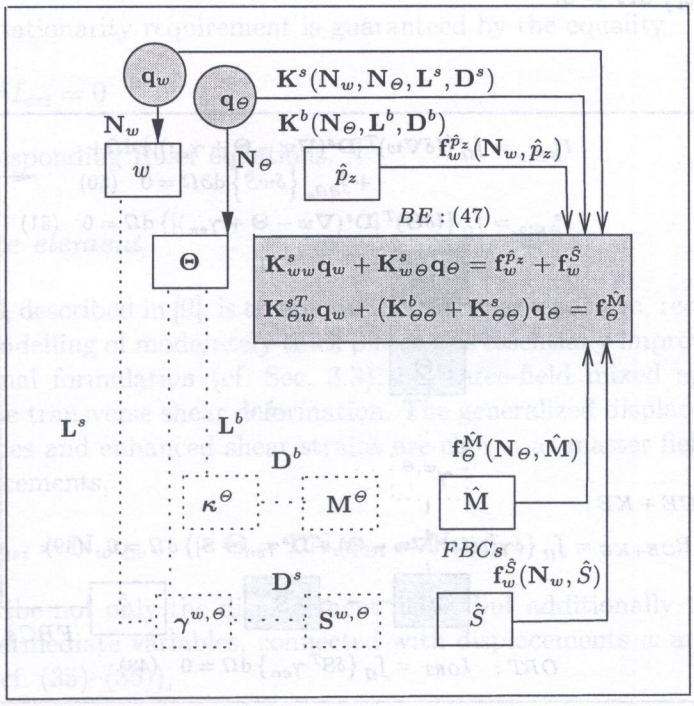


**Fig. 10.** Displacement FE model for bending and shear states in Mindlin–Reissner plate

leads to, according to the standard procedure, the following matrix equilibrium equations ($BE$), in which both bending and shear states are taken into account, with the use of displacement and rotational DOFs,

$$\left( \begin{bmatrix} \mathbf{0} & \mathbf{0} \\ \mathbf{0} & \mathbf{K}^{b}_{\Theta\Theta} \end{bmatrix} + \begin{bmatrix} \mathbf{K}^{s}_{ww} & \mathbf{K}^{s}_{w\Theta} \\ \mathbf{K}^{sT}_{\Theta w} & \mathbf{K}^{s}_{\Theta\Theta} \end{bmatrix} \right) \begin{bmatrix} \mathbf{q}_{w} \\ \mathbf{q}_{\Theta} \end{bmatrix} = \begin{bmatrix} \mathbf{f}^{\hat{p}_z}_{w} + \mathbf{f}^{\hat{S}}_{w} \\ \mathbf{f}^{\hat{\mathbf{M}}}_{\Theta} \end{bmatrix}. \tag{47}$$

The generalized displacements $w$, $\boldsymbol{\Theta}$, treated as master (primary) variables, are connected with secondary variables and the two sets of DOFs $\mathbf{q}_w$ , $\mathbf{q}_\Theta$ are calculated from two matrix equations. The corresponding graphic presentation is demonstrated by a diagram in Fig. 10.

### 5.3. Mixed formulation — displacement FE model for bending and EAS for shear states

To continue the discussion of Model Problem I, the description of the plate FE is presented in which generalized displacements, shear forces and enhanced shear strains are approximated. The weak formulations, presented in the subsequent subsections, can be considered as a starting point of FE modelling.

#### *5.3.1. Weighted residual form for EAS method for shear state*

Following the weighted residual formulation presented in Sec. 3.1 for a general case of three-field formulation, the integral forms for the shear state of Mindlin–Reissner plate can be derived [9, 11].

First of all, we must assure that the shear forces and additional enhanced shear strains are orthogonal to each other, hence the orthogonality integral condition

$$I_{ORT} = \int_{\Omega} \{\delta \mathbf{S}^{T} \boldsymbol{\gamma}_{en}\} \, \mathrm{d}\Omega = 0. \tag{48}$$

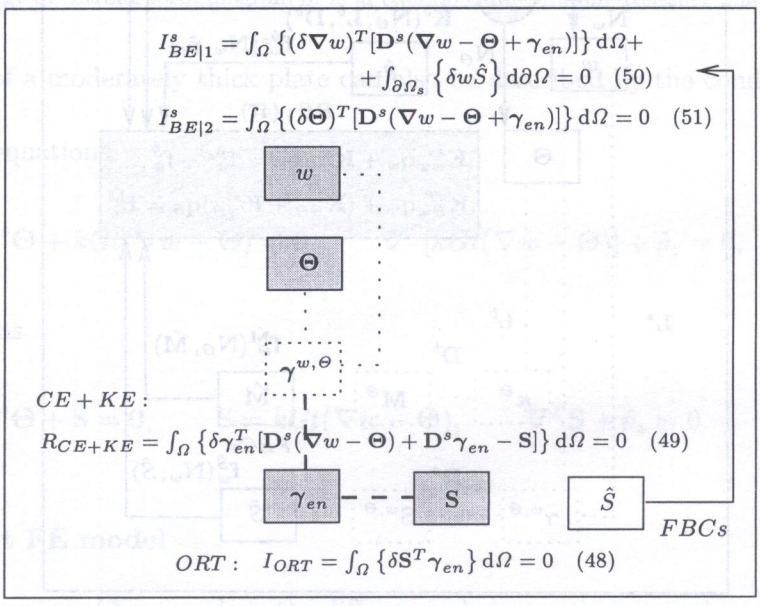


**Fig. 11.** Weighted residual form diagram for EAS shear formulation in Mindlin–Reissner plate

Next, three equations in their weak form can be obtained:

$$R^s_{CE+KE} = \int_\Omega \{\delta\boldsymbol{\gamma}^T_{en}[\mathbf{D}^s(\boldsymbol{\nabla} w - \boldsymbol{\Theta}) + \mathbf{D}^s\boldsymbol{\gamma}_{en} - \mathbf{S}]\}\,\mathrm{d}\Omega = 0, \tag{49}$$

$$I^s_{BE|1} = \int_\Omega \{(\delta\boldsymbol{\nabla} w)^T[\mathbf{D}^s(\boldsymbol{\nabla} w - \boldsymbol{\Theta} + \boldsymbol{\gamma}_{en})]\}\,\mathrm{d}\Omega + \int_{\partial\Omega_s}\left\{\delta w\hat{S}\right\}\mathrm{d}\partial\Omega = 0, \tag{50}$$

$$I^s_{BE|2} = \int_\Omega \{(\delta\boldsymbol{\Theta})^T[\mathbf{D}^s(\boldsymbol{\nabla} w - \boldsymbol{\Theta} + \boldsymbol{\gamma}_{en})]\}\,\mathrm{d}\Omega = 0. \tag{51}$$

The work of area load $\hat{p}_z$ and boundary loads $\hat{\mathbf{M}}$ is omitted here, but these loads will be included in the description of bending state. In Fig. 11 the above integral equations related to the shear state are treated as weakened links, marked by dashed lines.

### 5.3.2. *Variational form of $I^b_P + I^s_{HWen} - I_{ext}$ functional for bending and shear states*

Taking into account both the bending and shear states, as a second variant of the energy formulation the sum of potential energy functional $I^b_P[w, \boldsymbol{\Theta}]$ and the modified Hu–Washizu functional $I^s_{HWen}[w, \boldsymbol{\Theta}, \mathbf{S}, \boldsymbol{\gamma}_{en}]$, related to the EAS approach for the shear state, is adopted,

$$I[w, \boldsymbol{\Theta}, \mathbf{S}, \boldsymbol{\gamma}_{en}] = I^b_P + I^s_{HWen} - I_{ext} \tag{52}$$

$$\begin{aligned} &= \int_\Omega \left\{\frac{1}{2}(\boldsymbol{\nabla}^b\boldsymbol{\Theta})^T\mathbf{D}^b(\boldsymbol{\nabla}^b\boldsymbol{\Theta})\right\}\mathrm{d}\Omega \\ &\quad + \int_\Omega \left\{\frac{1}{2}(\boldsymbol{\nabla}\mathbf{w} - \boldsymbol{\Theta} + \boldsymbol{\gamma}_{en})^T\mathbf{D}^s(\boldsymbol{\nabla}\mathbf{w} - \boldsymbol{\Theta} + \boldsymbol{\gamma}_{en})\right\}\mathrm{d}\Omega \\ &\quad - \int_\Omega \{\mathbf{S}^T\boldsymbol{\gamma}_{en}\}\,\mathrm{d}\Omega - \int_\Omega \{w\hat{p}_z\}\,\mathrm{d}\Omega - \int_{\partial\Omega_s}\left\{w\hat{S}\right\}\mathrm{d}\partial\Omega - \int_{\partial\Omega_s}\left\{\boldsymbol{\Theta}^T\hat{\mathbf{M}}\right\}\mathrm{d}\partial\Omega. \end{aligned} \tag{53}$$

The satisfaction of stationarity requirement is guaranteed by the equality

$$\delta I^b_P + \delta I^s_{HWen} - \delta I_{ext} = 0 \tag{54}$$

which gives the corresponding Euler equations.

### 5.3.3. *QUAD plate element*

The QUAD plate FE, described in [9], is treated in this paper as a pattern, recommendable, low order finite element. FE modelling of moderately thick plates was essentially improved due to the adoption of modified variational formulation (cf. Sec. 3.3), i.e. three-field mixed approach with the EAS method related to the transverse shear deformation. The generalized displacements (deflections and rotations), shear forces and enhanced shear strains are chosen as master fields. The approximation of generalized displacements,

$$\mathbf{u} = \{w\} = \Sigma\mathbf{N}_i\mathbf{q}_{wi} = \mathbf{N}_w\mathbf{q}_w\,, \qquad \boldsymbol{\Theta} = \Sigma\mathbf{N}_i\mathbf{q}_{\Theta i} = \mathbf{N}_\Theta\mathbf{q}_\Theta\,, \tag{55}$$

is employed to describe not only the displacement fields, but additionally to calculate strains $\boldsymbol{\kappa}^\Theta$, $\boldsymbol{\gamma}^{w,\Theta}$, treated as intermediate variables, connected with displacements $w$ and rotations $\boldsymbol{\Theta}$, both in bending and shear (cf. (35)–(36)),

$$\boldsymbol{\kappa}^\Theta = \boldsymbol{\nabla}^b\mathbf{N}_\Theta\mathbf{q}_\Theta\,, \qquad \boldsymbol{\gamma}^{w,\Theta} = \boldsymbol{\nabla}\mathbf{N}_w\mathbf{q}_w - \mathbf{N}_\Theta\mathbf{q}_\Theta\,. \tag{56}$$

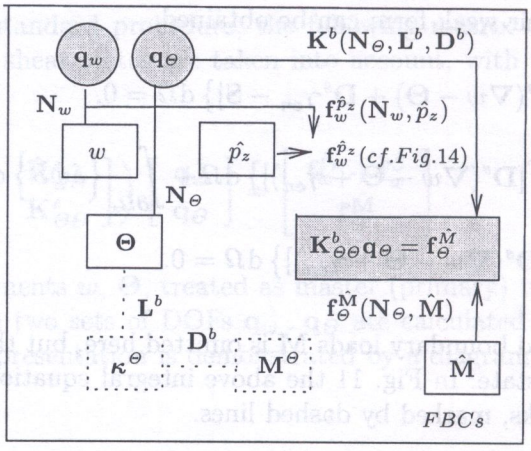


**Fig. 12.** Displacement FE model for bending state in Mindlin–Reissner plate

(i) In bending the displacement FE model is adopted, following the standard procedure (Sec. 5.2.2) with the calculation of stiffness matrix $\mathbf{K}^b_{\Theta\Theta}$ and vectors $\mathbf{f}^{\hat{p}}_w$, $\mathbf{f}^{\hat{\mathbf{M}}}_\Theta$; all relations between primary and secondary fields are graphically presented in Fig. 12.

(ii) In shear, beside the description of generalized displacements (55), the approximation of shear stresses and strains is essentially improved owing to the EAS concept (cf. Sec. 3 and in [9]), using the formulae

$$\mathbf{S} = \mathbf{N}_S\mathbf{q}_S = \mathbf{M}_S\mathbf{q}_S\,, \qquad \gamma_{en} = \mathbf{N}_{\gamma,en}\mathbf{q}_\gamma = \mathbf{M}_\gamma\mathbf{q}_\gamma\,, \tag{57}$$

with matrices $\mathbf{M}_S$, $\mathbf{M}_\gamma$ defined in the global frame. Initially, the shape function matrices are selected,

$$\bar{\mathbf{M}}_S(\xi,\eta) = \begin{bmatrix} 1 & 0 & \eta & 0 \\ 0 & 1 & 0 & \xi \end{bmatrix}, \qquad \bar{\mathbf{M}}_\gamma(\xi,\eta) = \begin{bmatrix} \xi & 0 & \xi\eta & 0 \\ 0 & \eta & 0 & \xi\eta \end{bmatrix}, \tag{58}$$

for which the following relations must be satisfied in the isoparametric space,

$$\int_\Omega \{\bar{\mathbf{M}}_S^T\bar{\mathbf{M}}_\gamma\}\,\mathrm{d}\xi\mathrm{d}\eta = 0, \qquad \int_\Omega \bar{\mathbf{M}}_\gamma \mathrm{d}\xi\mathrm{d}\eta = 0. \tag{59}$$

The transformation of shape functions $\bar{\mathbf{M}}_S$ and $\bar{\mathbf{M}}_\gamma$ for stresses and strains from the parent isoparametric to the global frame (Fig. 13)

$$\mathbf{N}_S = \mathbf{M}_S = \mathbf{J}_0\bar{\mathbf{M}}_S(\xi,\eta), \qquad \mathbf{N}_{\gamma,en} = \mathbf{M}_\gamma = \frac{j_0}{j}\,\mathbf{J}_0^{-T}\bar{\mathbf{M}}_\gamma(\xi,\eta), \tag{60}$$

is taken into account, using the matrix

$$\mathbf{J} = \begin{bmatrix} \frac{\partial x}{\partial \xi} & \frac{\partial y}{\partial \xi} \\ \frac{\partial x}{\partial \eta} & \frac{\partial y}{\partial \eta} \end{bmatrix},$$

where

$$j(\xi,\eta) = \det\mathbf{J}, \qquad J_{ij0} = J_{ij}|_{\xi,\eta=0}\,, \qquad j_0 = \det\mathbf{J}_0\,. \tag{61}$$

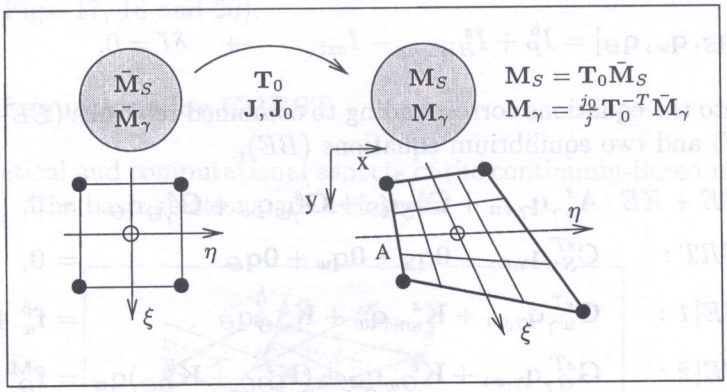


**Fig. 13.** Transformation of shape function matrices from isoparametric to global coordinate frame

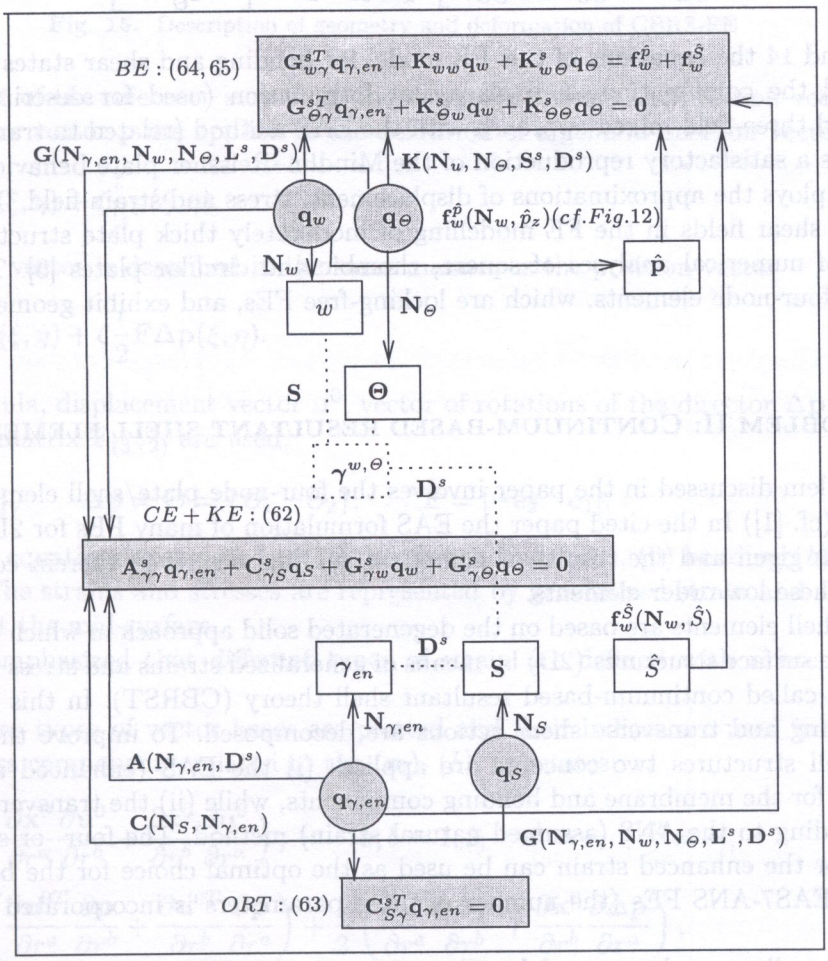


**Fig. 14.** Three-field FE model with EAS for shear state in the Mindlin–Reissner plate

(iii) All equations for the QUAD FE, related to bending and shear states, are derived from the functional given in Sec. 5.3.2. Following the general procedure stationarity conditions,

$$I = I[\mathbf{q}_{\gamma,en}, \mathbf{q}_S, \mathbf{q}_w, \mathbf{q}_\Theta] = I_P^b + I_{HWens}^s - I_{ext} \quad \rightarrow \quad \delta I = 0,$$

are developed into the equations corresponding to combined relations ($CE$+$KE$), orthogonality condition ($ORT$) and two equilibrium equations ($BE$),

$$\bigwedge \delta\mathbf{q}_{\gamma,en}: \quad CE+KE: \mathbf{A}_{\gamma\gamma}^s \mathbf{q}_{\gamma,en} + \mathbf{C}_{\gamma S}^s \mathbf{q}_S + \mathbf{G}_{\gamma w}^s \mathbf{q}_w + \mathbf{G}_{\gamma\Theta}^s \mathbf{q}_\Theta = \mathbf{0}, \tag{62}$$

$$\bigwedge \delta\mathbf{q}_S: \quad ORT: \quad \mathbf{C}_{S\gamma}^{sT} \mathbf{q}_{\gamma,en} + \mathbf{0}\mathbf{q}_S + \mathbf{0}\mathbf{q}_w + \mathbf{0}\mathbf{q}_\Theta = \mathbf{0}, \tag{63}$$

$$\bigwedge \delta\mathbf{q}_w: \quad BE|1: \quad \mathbf{G}_{w\gamma}^{sT} \mathbf{q}_{\gamma,en} + \mathbf{K}_{ww}^s \mathbf{q}_w + \mathbf{K}_{w\Theta}^s \mathbf{q}_\Theta = \mathbf{f}_w^{\hat{p}} + \mathbf{f}_w^{\hat{S}}, \tag{64}$$

$$\bigwedge \delta\mathbf{q}_\Theta: \quad BE|2: \quad \mathbf{G}_{\Theta\gamma}^{sT} \mathbf{q}_{\gamma,en} + \mathbf{K}_{\Theta w}^s \mathbf{q}_w + (\mathbf{K}_{\Theta\Theta}^s + \mathbf{K}_{\Theta\Theta}^b)\mathbf{q}_\Theta = \mathbf{f}_\Theta^{\hat{\mathbf{M}}}, \tag{65}$$

with their matrix form

$$\begin{bmatrix} \mathbf{A}_{\gamma\gamma}^s & \mathbf{C}_{\gamma S}^s & \mathbf{G}_{\gamma w}^s & \mathbf{G}_{\gamma\Theta}^s \\ \mathbf{C}_{S\gamma}^{sT} & \mathbf{0} & \mathbf{0} & \mathbf{0} \\ \mathbf{G}_{w\gamma}^{sT} & \mathbf{0} & \mathbf{K}_{ww}^s & \mathbf{K}_{w\Theta}^s \\ \mathbf{G}_{\Theta\gamma}^{sT} & \mathbf{0} & \mathbf{K}_{\Theta w}^s & (\mathbf{K}_{\Theta\Theta}^s + \mathbf{K}_{\Theta\Theta}^b) \end{bmatrix} \begin{bmatrix} \mathbf{q}_{\gamma,en} \\ \mathbf{q}_S \\ \mathbf{q}_w \\ \mathbf{q}_\Theta \end{bmatrix} = \begin{bmatrix} \mathbf{0} \\ \mathbf{0} \\ \mathbf{f}_w^{\hat{p}} + \mathbf{f}_w^{\hat{S}} \\ \mathbf{f}_\Theta^{\hat{\mathbf{M}}} \end{bmatrix}.$$

In Figs. 12 and 14 the equations of this FE model for bending and shear states are plotted.

In QUAD [9] the combination of displacement formulation (used for description of bending deformation) and three-field mixed approach with the EAS method (related to transverse shear deformation) yields a satisfactory reproduction of the Mindlin–Reissner plate behaviour. The applied methodology employs the approximations of displacement, stress and strain field. The introduction of the enhanced shear fields in the FE modelling of moderately thick plate structures gives satisfactory results of numerical analyses of square, rhombic and circular plates [9]. This is obtained using low order four-node elements, which are locking-free FEs, and exhibit geometrical distortion insensitivity.

## 6. Model problem II: Continuum-based resultant shell element

The second problem discussed in the paper involves the four-node plate/shell elements EAS4-ANS and EAS7-ANS (cf. [1]) In the cited paper the EAS formulation of many FEs for 2D, 3D, plate and shell structures is given and the results of numerical analysis described therein confirm the good performance of these low order elements.

These plate/shell elements are based on the degenerated solid approach in which continuum (3D) is reformulated to surface structures (2D) by means of generalized strains and stress resultants [7, 8]. This approach is called continuum-based resultant shell theory (CBRST). In this formulation the membrane, bending and transverse shear actions are decomposed. To improve the description of behaviour of shell structures two concepts are applied: (i) the EAS (enhanced assumed strain) approach is used for the membrane and bending components, while (ii) the transverse shear state is formulated according to the ANS (assumed natural strain) method. The four- or seven-parameter approximation for the enhanced strain can be used as the optimal choice for the bilinear so-called EAS4-ANS and EAS7-ANS FEs (the number of these parameters is incorporated in the name of the FE).

In order to describe membrane and bending state of shell FE briefly, the two-field formulation with enhanced strains was presented in Sec. 4, with a general idea presented in Sec. 2. For a comprehensive presentation of the issue and in order to define the notation (different in various papers [1, 7–9, 11]) the essential formulae from shell theory and main matrix definitions, together

with equations for this FE are discussed shortly below. The essential relations between membrane, bending and shear variables and the main features of the formulation are graphically presented in three new diagrams (Figs. 17, 18 and 20).

### 6.1. Strong form of equations for CBRST

All the detailed theoretical and computational aspects of the continuum-based resultant shell theory are presented in [7, 8]. The basic relations are as follows.

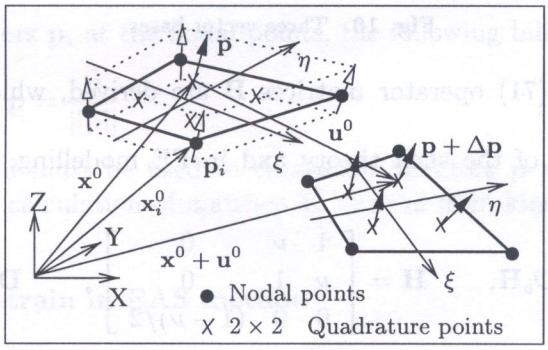


**Fig. 15.** Description of geometry and deformation of CBRS-FE

For every point of the reference surface in the structure domain the position vector $\mathbf{x}^0$ and the normalized director vector $\mathbf{p}$ are applied in the definition of a general position vector (Fig. 15)

$$\mathbf{x}(\xi,\eta,\zeta) = \mathbf{x}^0(\xi,\eta) + \zeta\frac{t}{2}\mathbf{p}(\xi,\eta). \tag{66}$$

The displacement vector is described in the same manner as the position vector

$$\mathbf{u}(\xi,\eta,\zeta) = \mathbf{u}^0(\xi,\eta) + \zeta\frac{t}{2}\mathbf{F}\Delta\mathbf{p}(\xi,\eta). \tag{67}$$

In the above formula, displacement vector $\mathbf{u}^0$, vector of rotations of the director $\Delta\mathbf{p}$, defined at the mid-surface, and matrix $\mathbf{F}_{(3\times2)}$ are used,

$$\mathbf{u}^0 = \{u_1\ u_2\ w\}, \qquad \Delta\mathbf{p} = \boldsymbol{\Theta} = \{\Theta_1 \quad \Theta_2\}, \qquad \mathbf{F} = [-\mathbf{e}_2 \quad \mathbf{e}_1]. \tag{68}$$

The kinematic equations are related to: (i) membrane (index $m$), (ii) bending ($b$) and (iii) shear ($s$) states [7–9]. The strains and stresses are represented by generalized strain and stress resultants vectors, defined at the mid-surface.

It should be emphasized that different types of strain are defined with reference to different vector bases.

In Fig. 16, three types of vector bases are plotted and their indices are used in the description of strain and stress components, related to the $(m)$, $(b)$, $(s)$ states:

$$\text{(i)}\quad \varepsilon_{ab} = \frac{1}{2}\left(\frac{\partial\mathbf{x}^0}{\partial r^a}\frac{\partial\mathbf{u}^0}{\partial r^b} + \frac{\partial\mathbf{x}^0}{\partial r^b}\frac{\partial\mathbf{u}^0}{\partial r^a}\right), \qquad (a,b=1,2;\quad r^1=r,\quad r^2=s), \tag{69}$$

$$\text{(ii)}\quad \kappa_{ab} = \frac{1}{2}\left(\frac{\partial\mathbf{u}^{0T}}{\partial r^a}\frac{\partial\mathbf{p}}{\partial r^b} + \frac{\partial\mathbf{u}^{0T}}{\partial r^b}\frac{\partial\mathbf{p}}{\partial r^a}\right) + \frac{1}{2}\left(\frac{\partial\mathbf{x}^0}{\partial r^a}\frac{\partial\Delta\mathbf{p}}{\partial r^b} + \frac{\partial\mathbf{x}^0}{\partial r^b}\frac{\partial\Delta\mathbf{p}}{\partial r^a}\right), \tag{70}$$

$$(a,b=1,2;\ r^1=r,\ r^2=s),$$

$$\text{(iii)}\quad \gamma_\alpha = \frac{\partial\mathbf{u}^{0T}}{\partial\xi^\alpha}\mathbf{p} + \frac{\partial\mathbf{x}^{0T}}{\partial\xi^\alpha}\Delta\mathbf{p}, \qquad (\alpha=1,2;\ \xi^1=\xi,\ \xi^2=\eta). \tag{71}$$

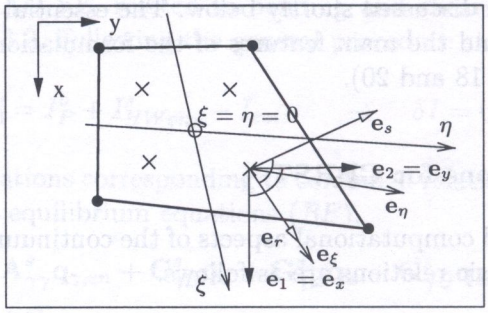


**Fig. 16.** Three vector bases

On the basis of Eqs. (69)–(71) operator matrices $\mathbf{B}$ are derived, which will be used in the FE kinematic relations.

In constitutive relations of the shell theory and in FE modelling, the following matrices are introduced:

$$\mathbf{D}^m = D_m \mathbf{H}, \qquad \mathbf{D}^b = D_b \mathbf{H}, \qquad \mathbf{H} = \begin{bmatrix} 1 & \nu & 0 \\ \nu & 1 & 0 \\ 0 & 0 & (1-\nu)/2 \end{bmatrix}, \qquad \mathbf{D}^s = D_s \begin{bmatrix} 1 & 0 \\ 0 & 1 \end{bmatrix}, \tag{72}$$

$$D_m = \frac{Et}{(1-\nu^2)}, \qquad D_b = \frac{t^2}{12} D_m, \qquad D_s = kGt.$$

In FE models, where the generalized displacements are approximated among other fields, the external work $I_{ext}$ is the place in the formulation where the prescribed area load vector $\hat{\mathbf{p}} = \{\hat{p}_1\ \hat{p}_2\ \hat{p}_n\}$ and boundary load vectors $\hat{\mathbf{t}}^m = \{\hat{\mathbf{N}}\} = \{\hat{N}_\nu\ \hat{N}_{\nu s}\}$, $\hat{\mathbf{t}}^b = \{\hat{\mathbf{M}}\} = \{\hat{M}_\nu\ \hat{M}_{\nu s}\}$ and $\hat{\mathbf{t}}^s = \{\hat{S}_\nu\}$ can be taken into account.

### 6.2. Geometry of EAS-ANS plate/shell elements

According to the isoparametric formulation, the description of FE geometry and displacement field are performed using the same approximation base functions, with standard unit square mapped to the shell element configuration,

$$\mathbf{x}(\xi,\eta,\zeta) = \sum \mathbf{N}_i(\xi,\eta)\, \mathbf{x}_i^0 + \sum \mathbf{N}_i(\xi,\eta)\, \zeta \frac{t_i}{2} \mathbf{p}_i, \tag{73}$$

$$\mathbf{x}_i^0 = \begin{bmatrix} (x_{it} + x_{ib})/2 \\ (y_{it} + y_{ib})/2 \\ (z_{it} + z_{ib})/2 \end{bmatrix}, \qquad \mathbf{p}_i = \frac{1}{t_i} \begin{bmatrix} x_{it} - x_{ib} \\ y_{it} - y_{ib} \\ z_{it} - z_{ib} \end{bmatrix},$$

$$\mathbf{u}(\xi,\eta,\zeta) = \sum \mathbf{N}_i(\xi,\eta)\, \mathbf{q}_{ui} + \sum \mathbf{N}_i(\xi,\eta)\, \zeta \frac{t_i}{2} \mathbf{F}_i \mathbf{q}_{\Theta i}, \tag{74}$$

$$\mathbf{q}_{ui} = \{u_i\ v_i\ w_i\}, \qquad \mathbf{q}_{\Theta i} = \{\Theta_{1i}\ \Theta_{2i}\}, \qquad \mathbf{F}_i = [-\mathbf{e}_{2i}\ \mathbf{e}_{1i}] = \left[ -\frac{\mathbf{V}_{2i}}{||\mathbf{V}_{2i}||} \ \frac{\mathbf{V}_{1i}}{||\mathbf{V}_{1i}||} \right],$$

index $t$ denoting the upper surface and $b$ the lower one.

The following vector bases $(\mathbf{e}_\xi, \mathbf{e}_\eta)$, $(\mathbf{e}_r, \mathbf{e}_s)$ are introduced in the FE domain (Fig. 16), in particular at quadrature points,

$$\mathbf{e}_\xi = \frac{\partial \mathbf{x}}{\partial \xi}, \qquad \mathbf{e}_\eta = \frac{\partial \mathbf{x}}{\partial \eta}, \tag{75}$$

$$\mathbf{e}_r = \frac{\partial \mathbf{x}}{\partial r}, \qquad \mathbf{e}_s = \frac{\partial \mathbf{x}}{\partial s}, \tag{76}$$

$$\mathbf{e}_r = \mathbf{e}_\xi\,, \qquad \mathbf{e}_t = \frac{\mathbf{e}_\xi \times \mathbf{e}_\eta}{||\mathbf{e}_\xi \times \mathbf{e}_\eta||}\,, \qquad \mathbf{e}_s = \mathbf{e}_t \times \mathbf{e}_r\,, \tag{77}$$

and base $(\mathbf{e}_{1i}\,,\, \mathbf{e}_{2i})$ at nodal points,

$$\begin{aligned}
&\mathbf{V}_{3i} \;= t_i \mathbf{p}_i\,,\\
&\mathbf{V}_{1i}: \quad \Delta x = \sum N_{i,\xi} x_i \Delta\xi, \quad \Delta y = \sum N_{i,\xi} y_i \Delta\xi, \quad \Delta z = \sum N_{i,\xi} z_i \Delta\xi, \quad \mathbf{e}_{1i} = \frac{\mathbf{V}_{1i}}{||\mathbf{V}_{1i}||}\,,\\
&\mathbf{V}_{2i} \;= \mathbf{V}_{3i} \times \mathbf{V}_{1i}\,, \quad \mathbf{e}_{2i} = \frac{\mathbf{V}_{2i}}{||\mathbf{V}_{2i}||}\,.
\end{aligned} \tag{78}$$

Using unit director vectors $\mathbf{p}_i$ at the nodal points, the following bilinear interpolation,

$$\tilde{\mathbf{p}}(\xi,\eta) = \sum \mathbf{N}_i \mathbf{p}_i\,, \qquad \mathbf{p} = \frac{\tilde{\mathbf{p}}}{||\tilde{\mathbf{p}}||}\,, \tag{79}$$

gives the director field, and must be used to determine directors $\mathbf{p}$ at Gauss quadrature points. Vectors $\mathbf{p}$ are useful in the calculation of matrices $\mathbf{L}$, derived from kinematic relations (70)–(71).

### 6.3. Approximation of strain in EAS method

The EAS formulation is applied for the membrane $(m)$ and bending $(b)$ states. The approximation of the strain field, composed of two parts, is proposed

$$\text{(i)}\quad \varepsilon^a_u = \mathbf{L}^a_u \mathbf{u} = (\mathbf{L}^a_u \mathbf{N}_u)\mathbf{q}_u = \mathbf{B}^a_u \mathbf{q}_u\,, \qquad \text{(ii)}\quad \boldsymbol{\varepsilon}^a_{en} = \mathbf{M}^a_\varepsilon \mathbf{q}_{\varepsilon,en}\,, \qquad \text{with indices } a = m, b.$$

Initially, the matrix $\bar{\mathbf{M}}^a_\varepsilon$ is adopted, with four or seven columns, according to the four- or seven-parameter approximation

$$\bar{\mathbf{M}}^a_\varepsilon = \left[\begin{array}{cccc|ccc} \xi & 0 & 0 & 0 & \xi\eta & 0 & 0 \\ 0 & \eta & 0 & 0 & 0 & \xi\eta & 0 \\ 0 & 0 & \xi & \eta & 0 & 0 & \xi\eta \end{array}\right].$$

The matrix $\bar{\mathbf{M}}^a_\varepsilon$ must be mapped from the isoparametric to Cartesian space using the transformation

$$\mathbf{M}^a_\varepsilon = \frac{j_0}{j}\,\mathbf{T}_0^{-T} \bar{\mathbf{M}}^a_\varepsilon\,.$$

Next, the matrix $\mathbf{T}_0$ in its standard form is computed at the central point $(\xi = \eta = 0)$ of the FE domain as

$$\mathbf{T}_0 = \left[\begin{array}{ccc} J^2_{110} & J^2_{210} & 2J_{110}J_{210} \\ J^2_{120} & J^2_{220} & 2J_{120}J_{220} \\ J_{110}J_{120} & J_{210}J_{220} & J_{110}J_{220} + J_{120}J_{210} \end{array}\right].$$

Considering the problem in the $(\mathbf{e}_r\,,\, \mathbf{e}_s)$ base, matrix $\mathbf{T}^{(rs-\xi\eta)}$ must be calculated,

$$\mathbf{T}^{(rs-\xi\eta)} = \left[\begin{array}{cc} \frac{\partial \mathbf{x}}{\partial \xi}\frac{\partial \mathbf{x}^T}{\partial r} & \frac{\partial \mathbf{x}}{\partial \xi}\frac{\partial \mathbf{x}^T}{\partial s} \\ \frac{\partial \mathbf{x}}{\partial \eta}\frac{\partial \mathbf{x}^T}{\partial r} & \frac{\partial \mathbf{x}}{\partial \eta}\frac{\partial \mathbf{x}^T}{\partial s} \end{array}\right] = \left[\begin{array}{cc} \frac{\partial r}{\partial \xi} & \frac{\partial s}{\partial \xi} \\ \frac{\partial r}{\partial \eta} & \frac{\partial s}{\partial \eta} \end{array}\right],$$

which is next used to transform the derivatives of shape functions,

$$\left[\begin{array}{c} N^n_{,r} \\ N^n_{,s} \end{array}\right] = \left[\begin{array}{cc} \frac{\partial r}{\partial \xi} & \frac{\partial s}{\partial \xi} \\ \frac{\partial r}{\partial \eta} & \frac{\partial s}{\partial \eta} \end{array}\right]^{-1} \left[\begin{array}{c} N^n_{,\xi} \\ N^n_{,\eta} \end{array}\right] = [\mathbf{T}^{(rs-\xi\eta)}]^{-1} \left[\begin{array}{c} N^n_{,\xi} \\ N^n_{,\eta} \end{array}\right], \qquad n = 1,2,3,4,$$

and to calculate the new matrix $\mathbf{T}_0$, with elements $J_{ij0}$ replaced by $T^{(rs-\xi\eta)}_{ij0}$.

### *6.3.1. EAS model for membrane state*

Now, detailed relations for the description of the strain field in the membrane state are cited. The strains are related to the $(\mathbf{e}_r\,,\,\mathbf{e}_s)$ base and composed of two parts, after the EAS method:

(i) displacement-gradients strains, cf. Eq. (69),

$$\boldsymbol{\varepsilon}_u^m = \boldsymbol{\varepsilon}^u = \begin{bmatrix} \varepsilon_{rr} \\ \varepsilon_{ss} \\ \varepsilon_{rs} \end{bmatrix} = \mathbf{L}_u^m \mathbf{u} = \mathbf{B}_u^m \mathbf{q}_u + \mathbf{B}_\Theta^m \mathbf{q}_\Theta = \begin{bmatrix} \mathbf{B}_u^m & \mathbf{0} \end{bmatrix} \begin{bmatrix} \mathbf{q}_u \\ \mathbf{q}_\Theta \end{bmatrix}, \tag{80}$$

(ii) enhanced strains,

$$\boldsymbol{\varepsilon}_{en}^m = \boldsymbol{\varepsilon}_{en} = \mathbf{N}_{\varepsilon,en}\mathbf{q}_{\varepsilon,en} = \mathbf{M}_\varepsilon^m \mathbf{q}_{\varepsilon,en}\,, \qquad \mathbf{N}_{\varepsilon,en} = \mathbf{M}_\varepsilon^m\,, \tag{81}$$

with

$$\mathbf{L}_u^m = \begin{bmatrix} \frac{\partial \mathbf{x}^0}{\partial r}\frac{\partial}{\partial r} \\ \frac{\partial \mathbf{x}^0}{\partial s}\frac{\partial}{\partial s} \\ \frac{\partial \mathbf{x}^0}{\partial r}\frac{\partial}{\partial s} + \frac{\partial \mathbf{x}^0}{\partial s}\frac{\partial}{\partial r} \end{bmatrix}, \qquad \mathbf{L}_\Theta^m = \mathbf{0}, \qquad \mathbf{B}_\Theta^m = \mathbf{0}, \qquad \mathbf{B}^m = \begin{bmatrix} \mathbf{B}_u^m & \mathbf{0} \end{bmatrix}. \tag{82}$$

Matrix $\mathbf{D}^m$, known from the constitutive relations, will also be used in further definitions.

For the membrane state two matrix equations are

$$\bigwedge \delta\mathbf{q}_{\varepsilon,en}: \qquad \mathbf{A}_{\varepsilon\varepsilon}^m \mathbf{q}_{\varepsilon,en} + \mathbf{G}_{\varepsilon u}^m \mathbf{q}_u = \mathbf{0}, \tag{83}$$

$$\bigwedge \delta\mathbf{q}_u: \qquad \mathbf{G}_{u\varepsilon}^{mT} \mathbf{q}_{\varepsilon,en} + \mathbf{K}_{uu}^m \mathbf{q}_u = \mathbf{f}_u^{\hat{\mathbf{p}}} + \mathbf{f}_u^{\hat{\mathbf{N}}}, \tag{84}$$

where

$$\mathbf{K}_{uu}^m = \int_{\Omega_e} \{(\mathbf{B}_u^m)^T \mathbf{D}^m \mathbf{B}_u^m\}\,\mathrm{d}\Omega,$$

$$\mathbf{A}_{\varepsilon\varepsilon}^m = \int_{\Omega_e} \{\mathbf{M}_\varepsilon^{mT} \mathbf{D}^m \mathbf{M}_\varepsilon^m\}\,\mathrm{d}\Omega,$$

$$\mathbf{G}_{\varepsilon u}^m = \int_{\Omega_e} \{\mathbf{M}_\varepsilon^{mT} \mathbf{D}^m \mathbf{B}_u^m\}\,\mathrm{d}\Omega,$$

$$\mathbf{f}_u^{\hat{\mathbf{p}}} = \int_{\Omega_e} \{\mathbf{N}_u^T \hat{\mathbf{p}}\}\,\mathrm{d}\Omega, \qquad \mathbf{f}_u^{\hat{\mathbf{N}}} = \int_{\partial\Omega_{e,s}} \left\{\mathbf{N}_u^T \hat{\mathbf{N}}\right\}\mathrm{d}\partial\Omega.$$

The modified stiffness matrix $\mathbf{K}_{uu}^{m*}$ is calculated using the following formula, ensuing from the condensation of the enhanced strain parameters

$$\mathbf{K}_{uu}^{m*} = \mathbf{K}_{uu}^m - \mathbf{G}^{mT}(\mathbf{A}^m)^{-1}\mathbf{G}^m.$$

Having modified the general diagram for the two-field FE model with EAS (Fig. 7), the diagram for membrane state of the plate/shell FE is plotted (Fig. 17).

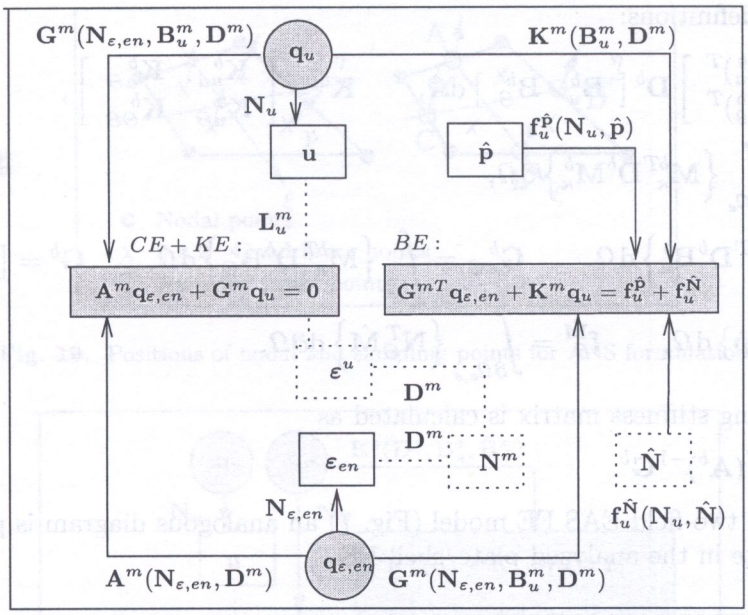


**Fig. 17.** EAS model ($\mathbf{u} - \boldsymbol{\varepsilon}_{en}$) for membrane state in plate/shell FE

### *6.3.2. EAS model for bending state*

Analogous to the membrane state, now the local orthogonal co-ordinate system $(\mathbf{e}_r, \mathbf{e}_s)$ is used for the bending state. The kinematic relations are

$$\boldsymbol{\varepsilon}_u^b = \boldsymbol{\kappa}^{u\Theta} = \begin{bmatrix} \kappa_{rr} \\ \kappa_{ss} \\ \kappa_{rs} \end{bmatrix} = \mathbf{L}_u^b\mathbf{u} + \mathbf{L}_\Theta^b\boldsymbol{\Theta} = \mathbf{B}_u^b\mathbf{q}_u + \mathbf{B}_\Theta^b\mathbf{q}_\Theta = \begin{bmatrix} \mathbf{B}_u^b & \mathbf{B}_\Theta^b \end{bmatrix} \begin{bmatrix} \mathbf{q}_u \\ \mathbf{q}_\Theta \end{bmatrix}, \tag{85}$$

with

$$\mathbf{L}_u^b = \begin{bmatrix} \frac{\partial \mathbf{p}^T}{\partial r}\frac{\partial}{\partial r} \\ \frac{\partial \mathbf{p}^T}{\partial s}\frac{\partial}{\partial s} \\ \frac{\partial \mathbf{p}^T}{\partial r}\frac{\partial}{\partial s} + \frac{\partial \mathbf{p}^T}{\partial s}\frac{\partial}{\partial r} \end{bmatrix}, \qquad \mathbf{L}_\Theta^b = \begin{bmatrix} \frac{\partial \mathbf{x}^0}{\partial r}\frac{\partial}{\partial r} \\ \frac{\partial \mathbf{x}^0}{\partial s}\frac{\partial}{\partial s} \\ \frac{\partial \mathbf{x}^0}{\partial r}\frac{\partial}{\partial s} + \frac{\partial \mathbf{x}^0}{\partial s}\frac{\partial}{\partial r} \end{bmatrix} \cdot \mathbf{T}_\Theta^{(g-n)}, \qquad \mathbf{B}^b = \begin{bmatrix} \mathbf{B}_u^b & \mathbf{B}_\Theta^b \end{bmatrix}$$

and additional enhanced bending strains are interpolated

$$\boldsymbol{\varepsilon}_{en}^b = \boldsymbol{\kappa}_{en} = \mathbf{N}_{\kappa,en}\mathbf{q}_{\kappa,en} = \mathbf{M}_\kappa^b\mathbf{q}_{\kappa,en}\,, \qquad \mathbf{N}_{\kappa,en} = \mathbf{M}_\kappa^b\,. \tag{86}$$

In the bending state matrix $\mathbf{D}^b$ will also be employed

$$\mathbf{D}^b = \frac{t^2}{12}\mathbf{D}^m.$$

In the EAS FE model, with displacement and rotational nodal DOFs and strain parameters, three equations are

$$\bigwedge \delta\mathbf{q}_{\kappa,en}: \qquad \mathbf{A}_{\kappa\kappa}^b\mathbf{q}_{\kappa,en} + \mathbf{G}_{\kappa u}^b\mathbf{q}_u + \mathbf{G}_{\kappa\Theta}^b\mathbf{q}_\Theta = \mathbf{0}, \tag{87}$$

$$\bigwedge \delta\mathbf{q}_u: \qquad \mathbf{G}_{u\kappa}^{bT}\mathbf{q}_{\kappa,en} + \mathbf{K}_{uu}^b\mathbf{q}_u + \mathbf{K}_{u\Theta}^b\mathbf{q}_\Theta = \mathbf{f}_u^{\hat{\mathbf{p}}}\,, \tag{88}$$

$$\bigwedge \delta\mathbf{q}_\Theta: \qquad \mathbf{G}_{\Theta\kappa}^{bT}\mathbf{q}_{\kappa,en} + \mathbf{K}_{\Theta u}^b\mathbf{q}_u + \mathbf{K}_{\Theta\Theta}^b\mathbf{q}_\Theta = \mathbf{f}_\Theta^{\hat{\mathbf{M}}}, \tag{89}$$

with the following definitions:

$$\mathbf{K}^b = \int_{\Omega_e} \begin{bmatrix} (\mathbf{B}_u^b)^T \\ (\mathbf{B}_\theta^b)^T \end{bmatrix} \mathbf{D}^b \begin{bmatrix} \mathbf{B}_u^b & \mathbf{B}_\Theta^b \end{bmatrix} \mathrm{d}\Omega, \qquad \mathbf{K}^b = \begin{bmatrix} \mathbf{K}_{uu}^b & \mathbf{K}_{u\Theta}^b \\ \mathbf{K}_{u\Theta}^b & \mathbf{K}_{\Theta\Theta}^b \end{bmatrix},$$

$$\mathbf{A}^b = \mathbf{A}_{\kappa\kappa}^b = \int_{\Omega_e} \left\{ \mathbf{M}_\kappa^{bT} \mathbf{D}^b \mathbf{M}_\kappa^b \right\} \mathrm{d}\Omega,$$

$$\mathbf{G}_{\kappa u}^b = \int_{\Omega_e} \left\{ \mathbf{M}_\kappa^{bT} \mathbf{D}^b \mathbf{B}_u^b \right\} \mathrm{d}\Omega, \qquad \mathbf{G}_{\kappa\Theta}^b = \int_{\Omega_e} \left\{ \mathbf{M}_\kappa^{bT} \mathbf{D}^b \mathbf{B}_\Theta^b \right\} \mathrm{d}\Omega, \qquad \mathbf{G}^b = \begin{bmatrix} \mathbf{G}_{\kappa u}^b & \mathbf{G}_{\kappa\Theta}^b \end{bmatrix},$$

$$\mathbf{f}_u^{\hat{\mathbf{p}}} = \int_{\Omega_e} \left\{ \mathbf{N}_u^T \hat{\mathbf{p}} \right\} \mathrm{d}\Omega, \qquad \mathbf{f}_\Theta^{\hat{\mathbf{M}}} = \int_{\partial\Omega_{e,s}} \left\{ \mathbf{N}_\Theta^T \hat{\mathbf{M}} \right\} \mathrm{d}\partial\Omega.$$

The modified bending stiffness matrix is calculated as

$$\mathbf{K}^{b*} = \mathbf{K}^b - \mathbf{G}^{bT} (\mathbf{A}^b)^{-1} \mathbf{G}^b.$$

According to the two-field EAS FE model (Fig. 7) an analogous diagram is presented in Fig. 18 for the bending state in the analyzed plate/shell FE.

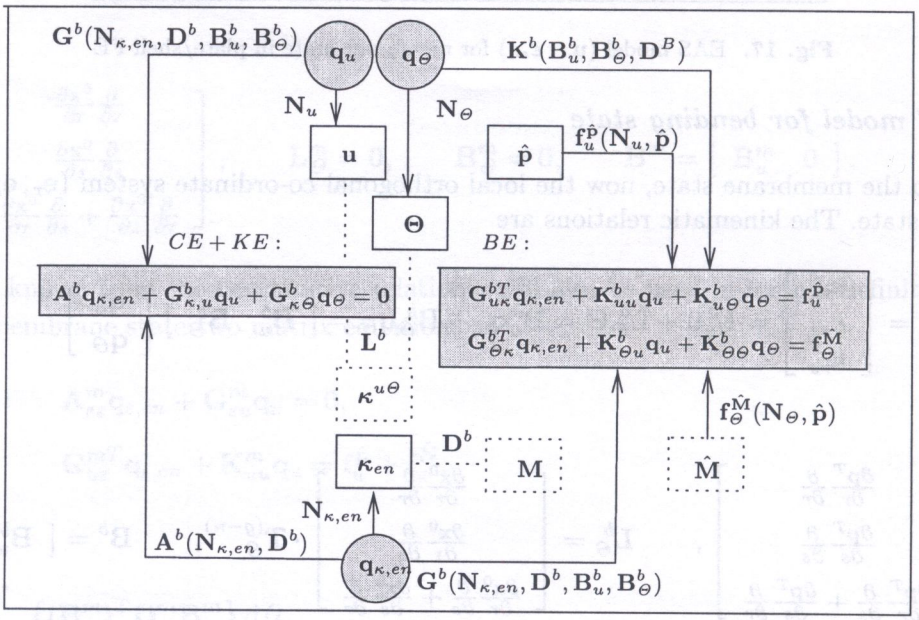


**Fig. 18.** EAS model ($\mathbf{u} - \boldsymbol{\kappa}_{en}$) for bending state in plate/shell FE

### 6.4. ANS model for shear state

The transverse shear strain representation is designed according to the ANS method. The vectors $(\mathbf{e}_\xi, \mathbf{e}_\eta)$ of the natural coordinate system are adopted in the description of the shear strains. The following formulae are derived,

$$\boldsymbol{\varepsilon}_u^s = \boldsymbol{\gamma}^{u\Theta} = \begin{bmatrix} \gamma_\xi \\ \gamma_\eta \end{bmatrix} = \mathbf{L}_u^s \mathbf{u} + \mathbf{L}_\Theta^s \boldsymbol{\Theta} = \mathbf{B}_u^s \mathbf{q}_u + \mathbf{B}_\Theta^s \mathbf{q}_\Theta = \begin{bmatrix} \mathbf{B}_u^s & \mathbf{B}_\Theta^s \end{bmatrix} \begin{bmatrix} \mathbf{q}_u \\ \mathbf{q}_\Theta \end{bmatrix}, \tag{90}$$

with

$$\mathbf{L}_u^s = \begin{bmatrix} \mathbf{p}^T \frac{\partial}{\partial \xi} \\ \mathbf{p}^T \frac{\partial}{\partial \eta} \end{bmatrix}, \qquad \mathbf{L}_\Theta^s = \begin{bmatrix} \frac{\partial x}{\partial \xi} \\ \frac{\partial x}{\partial \eta} \end{bmatrix} \cdot \mathbf{T}_\Theta^{(g-n)}, \qquad \mathbf{B}^s = \begin{bmatrix} \mathbf{B}_u^s & \mathbf{B}_\Theta^s \end{bmatrix}.$$

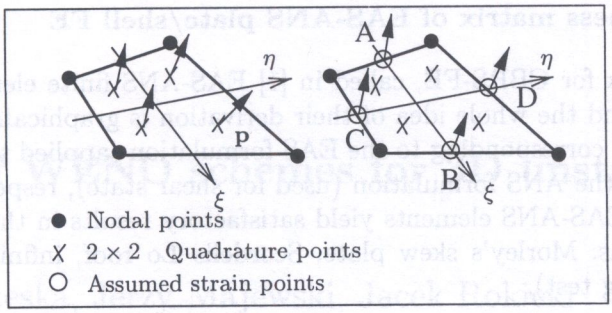


**Fig. 19.** Positions of nodal and sampling points for ANS formulation

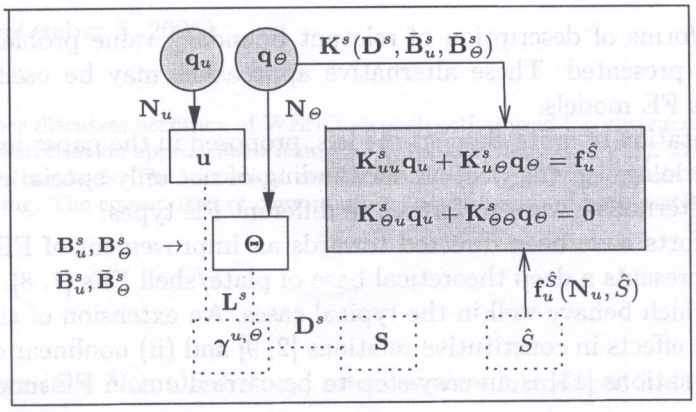


**Fig. 20.** ANS formulation for shear state in plate/shell FE

Firstly, the covariant transverse shear strains are calculated at the midpoints of element boundaries, i.e. components $\gamma_\xi$ are obtained at sampling points A and B (Fig. 19) and components $\gamma_\eta$ at points C and D. Secondly, constant-linear fields $\bar{\gamma}_\xi$ and $\bar{\gamma}_\eta$ are defined on the basis of two relevant points

$$\bar{\gamma}_\xi = \frac{1}{2}(1-\eta)\gamma^A_\xi + \frac{1}{2}(1+\eta)\gamma^B_\xi, \tag{91}$$

$$\bar{\gamma}_\eta = \frac{1}{2}(1-\xi)\gamma^C_\eta + \frac{1}{2}(1+\xi)\gamma^D_\eta. \tag{92}$$

This way the $\bar{\mathbf{B}}^s_u$ and $\bar{\mathbf{B}}^s_\Theta$ matrices are calculated and used to determine the stiffness matrix for the shear state

$$\mathbf{K}^s = \int_{\Omega_e} \begin{bmatrix} (\bar{\mathbf{B}}^s_u)^T \\ (\bar{\mathbf{B}}^s_\Theta)^T \end{bmatrix} \mathbf{D}^s \begin{bmatrix} \bar{\mathbf{B}}^s_u & \bar{\mathbf{B}}^s_\Theta \end{bmatrix} \mathrm{d}\Omega, \quad \mathbf{K}^s = \begin{bmatrix} \mathbf{K}^s_{uu} & \mathbf{K}^s_{u\Theta} \\ \mathbf{K}^s_{u\Theta} & \mathbf{K}^s_{\Theta\Theta} \end{bmatrix},$$

from which two matrix equations are derived

$$\bigwedge \delta\mathbf{q}_u: \qquad \mathbf{K}^s_{uu}\mathbf{q}_u + \mathbf{K}^s_{u\Theta}\mathbf{q}_\Theta = \mathbf{f}^{\hat{S}}_u, \tag{93}$$

$$\bigwedge \delta\mathbf{q}_\Theta: \qquad \mathbf{K}^s_{\Theta u}\mathbf{q}_u + \mathbf{K}^s_{\Theta\Theta}\mathbf{q}_\Theta = \mathbf{0}, \tag{94}$$

where additionally the following vector appears,

$$\mathbf{f}^{\hat{S}}_u = \int_{\partial\Omega_{e,s}} \left\{ \mathbf{N}^T_u \hat{S} \right\} \mathrm{d}\partial\Omega.$$

The diagram for the shear state (Fig. 20) has the same structure as the diagram for the displacement FE model, with the main differences: matrices $\bar{\mathbf{B}}^s_u$ and $\bar{\mathbf{B}}^s_\Theta$ are obtained in two steps, using two types of sampling points and with individual treatment of the two components of the shear strain vector.

### 6.5. Generalized stiffness matrix of EAS-ANS plate/shell FE

The final stiffness matrix for CBRS-FE, called in [1] EAS-ANS finite element, is obtained adding matrices $\mathbf{K}^m$, $\mathbf{K}^b$, $\mathbf{K}^s$, and the whole idea of their derivation is graphically presented in three diagrams in Figs. 17, 18, 20, corresponding to the EAS formulation (applied to describe the membrane and bending state), and the ANS formulation (used for shear state), respectively.

As shown in [1], the EAS-ANS elements yield satisfactory results in the computational analysis of the following problems: Morley's skew plate, Scordelis–Lo roof, infinitely long cylinder under constant bending (locking test).

## 7. Final remarks

Three mathematical forms of description of relevant boundary value problems: strong, weak and variational forms are presented. These alternative approaches may be used as the basis for the formulation of various FE models.

The graphic presentation of finite element models, proposed in the paper in conceptual diagrams, is a convincing methodology, giving deep understanding of not only special methodologies as EAS or ANS, but also of alternative ways to formulate different FE types.

For years many efforts have been directed towards an improvement of FE modelling of surface structures. Paper [1] presents a deep theoretical base of plate/shell FEs [7, 8]. The applied concepts give low-order FEs, which behave well in the typical cases. An extension of the EAS concept to incorporate: (i) inelastic effects in constitutive relations [2, 9] and (ii) nonlinear displacement-gradient terms in kinematic equations [11] is an easy step to be carried out in FE modelling.

## Acknowledgements

The author is indebted to Dr Jerzy Pamin for helpful remarks and discussions during the preparation of her paper.

## References

[1] U. Andelfinger, E. Ramm. EAS-elements for 2D, 3D, plate and shell structures and their equivalence to HR elements. *Int. J. Numer. Meth. Engng.*, **36**: 1311–1337, 1991.

[2] U. Andelfinger, E. Ramm, D. Roehl. 2D- and 3D-enhanced assumed strain element method, In: E. Oñate, D.R.J. Owen, eds., *Proc. 3rd Int. Conference on Computational Plasticity, Fundamentals and Applications*, Barcelona, April 1992. Pineridge Press, Swansea, 1992.

[3] C. Fellippa. *Advanced Finite Element Methods (ASEN 5367)*, Spring 2003, Course materials. Department of Aerospace Engineering Sciences, University of Colorado at Boulder, http://titan.colorado.edu/courses.d/AFEA.d/, 2003.

[4] M. Radwańska. Degenerated shell elements in the context of shell theories of first and second approximation, In: *Proc. 5th Conference on Shell Structures. Theory and applications*, Janowice, Oct. 1992.

[5] M. Radwańska, W. Gilewski. A survey of finite element for analysis of moderately thick shells. *Finite Elements Anal. Design*, **9**: 1–21, 1991.

[6] M. Radwańska. A survey of various FE models with conceptual diagrams for linear analysis. *Computer Assisted Mechanics and Engineering Sciences*, **13**: 209–223, 2006.

[7] J.C. Simo, D.D. Fox. On stress resultant geometrically exact shell model. Part I: Formulation and optimal parametrization. *Comp. Methods Appl. Mech. Engng.*, **72**: 267–304, 1989.

[8] J.C. Simo, D.D. Fox, M.S. Rifai. On stress resultant geometrically exact shell model. Part II: Computational aspects. *Comp. Methods Appl. Mech. Engng.*, **73**: 53–92, 1989.

[9] J.C. Simo, M.S. Rifai. A class of mixed assumed strain methods and method of incompatible modes. *Int. J. Numer. Meth. Engng.*, **29**: 1595–1638, 1990.

[10] N.E. Wiberg. On understanding and teaching of the finite element method. *Commun. Numer. Methods Engng.*, **11**: 105–115, 1995.

[11] O.C. Zienkiewicz, R.L. Taylor. *The Finite Element Method.* Butterworth-Heinemann, Oxford, fifth edition, 2000.